# DIRECT TORQUE CONTROLLED INDUCTION MOTOR DRIVE

***Thesis submitted in partial fulfillment of the requirements for the award of degree of***

**Master of Engineering**

**in**

**Power Systems & Electric Drives**

**Thapar University, Patiala**


By

**Abhishek Verma**

(Roll No: 800841001)

Under the supervision of

**Dr. Yogesh K. Chauhan**

**Assistant professor, EIED**

**ELECTRICAL AND INSTRUMENTATION ENGINEERING DEPARTMENT**

**THAPAR UNIVERSITY**

**PATIALA-147004**


**DECEMBER, 2010**

# CERTIFICATE

I hereby certify that the work which is being presented in this thesis entitled **"Direct Torque Controlled Induction Motor Drive"** in partial fulfillment of the requirements of the award of the degree of master of engineering in ***Power Systems & Electric Drives*** submitted in Electrical and Instrumentation Engineering Department of Thapar University, Patiala is an authentic record of my own work carried out under the supervision of **Dr. Yogesh K. Chauhan**, Asst. Prof., EIED.

The matter presented in this thesis has not been submitted by me for the award of any other degree of this or any other university.

Abhishek

**Abhishek Verma**

Roll No. 800841001

It is to certified that the above statement made by the student is correct to the best of our knowledge and belief.

**Dr. Yogesh K. Chauhan**

**Assistant Professor, EIED**

Thapar University, Patiala

**Countersigned by:**

**Dr. Smarajit Ghosh**

**Professor & Head, EIED**

Thapar University

Patiala

**Dr. S. K. Mohapatra**

**Dean of Academic Affairs**

Thapar University

Patiala



i

# ACKNOWLEDGMENT

Thesis work is completed with prayers of many and love of my family and friends. However, there are a few people that I would like to specially acknowledge and extend my heartfelt gratitude who have made the completion of this thesis work possible. With the biggest contribution to this report; I would like to thank my guide **Dr. Yogesh K. Chauhan, Assistant Prof., EIED** had given me his full encouragement and support in guiding me with stimulating suggestions and encouragement to go ahead in all the time of the thesis work.

I thank to **Dr. Smarajit Ghosh, Professor & Head, EIED** and **Dr. Yaduvir Singh, PG Co-Ordinator, EIED** for their continuos inspiration during this thesis work.

The paucity of words does not compromise for extending my thanks to all the staff members of EIED, Thapar University, my all family members and friends whose uninterrupted love, inspiration and blessings helped me in completing this research report.

At last but not the least my gratitude towards my parents, I would also like to thank God for not letting me down at the time of crisis and showing me the silver lining in the dark clouds.

(Abhishek Verma)

Roll No. 800841001

# ABSTRACT

In conventional Direct Torque Control (DTC), the selection of flux linkage and electromagnetic torque errors are made within the respective flux and torque hysteresis bands, in order to obtain fast torque response, low inverter switching frequency and low harmonic losses. However, DTC drives utilizing hysteresis comparators suffer from high torque ripple and variable switching frequency.

Space Vector Modulation (SVM) is the strategy to minimize the torque ripple of induction motor in which, the stator flux level is selected in accordance with the efficiency optimized motor performance. SVM method is incorporated with direct torque control (DTC-SVM) for induction motor drives. However, the basis of the DTC-SVM strategy is the calculation of the required voltage space vector to compensate the flux and torque errors exactly by using a predictive technique and then its generation using the SVM at each sample period.

In this thesis work, the simulation of different DTC schemes (Conventional DTC and DTC-SVM) has been carried out using MATLAB/SIMULINK and the results are compared.

# TABLE OF CONTENTS

# LIST OF FIGURES

# LIST OF TABLES

# CHAPTER 1

# INTRODUCTION

## 1.1 OVERVIEW

Direct torque control (DTC) drives are finding great interest, since ABB recently introduced the first industrial direct-torque-controlled induction motor drive in the mid-1980's, which according to ABB can work even at zero speed. This is a very significant industrial contribution, and it has been stated by ABB that ''DTC is the latest AC motor control method''. ABB has also introduced a DTC based medium voltage drive called the ACS1000, thus feeding pure sinusoidal voltages and currents to the motor. This is ideal for pumps and fans [3].

With the revolutionary DTC technology developed by ABB, field orientation is achieved without feedback using advanced motor theory to calculate the motor torque directly and without using pulse width modulation. The controlling variables are motor magnetizing flux and motor torque**.** With DTC there is no modulator and no requirement for a tachometer or position encoder to feed back the speed or position of the motor shaft. DTC uses the fastest digital signal processing hardware available. The result is a drive with a torque response that is typically 10 times faster than any AC or DC drive [1].

The Conventional DTC method yields slow response during start up and change in either direction of torque and flux. In addition to this, also high torque ripples are found. Several techniques have been developed to improve the torque performance. One of them is to reduce the ripples using SVM technique. SVM was first presented by a group of German researched in the second half of the 1980s. Since then, a lot of work has been done on the theory and implementation of SVM techniques. SVM techniques have several advantages such as, lower torque ripple, lower Total Harmonic Distortion (THD) in the AC motor current, lower switching losses, and easier to implement in the digital systems. At each cycle period, this SVM technique is used to obtain the voltage space vector required to exactly compensate the flux and torque errors. The torque ripples for this DTC-SVM is significantly reduced and switching frequency is maintained constant.

## 1.2 LITERATURE REVIEW

The literature on control of induction motor drive is very much diversified over the v controlling aspects the brief review is presented on the subject of new schemes with DTC in order of minimization of torque ripples with the DTC and other things.

Krause [1] gives an overview about the mathematical modeling of various machines including induction machine. The various reference frames and necessary transformations required for transferring the quantities from one reference frame to another has been studied. Bose [2] describes the steady state performance of induction motors followed by the dynamic d-q model in both synchronously rotating reference frame and stationary reference frame. Then, state-space equations in terms of flux linkages are derived mainly for simulation. The principle of the sinusoidal Pulse Width Modulation (PWM) with instantaneous current control has been explained Similarly, Rashid [3] presented in addition with vector control systems, an instantaneous torque control yielding very fast torque response can be obtained by employing direct torque control.

The DTC architecture allows the independent and decoupled control of torque and stator flux. The implementation of the DTC model has been deeply described and justified its realization using Simulink model [4]. Several simulations have been carried out in a steady state and transient operation on a speed control mode and also the torque control of an induction machine based on DTC strategy and a comprehensive study is presented [5]. An explanation of direct self control and the field-orientation concepts implemented in the adaptive motor model block is presented, dealing with the basic concepts behind direct torque control [6].

Among all control methods for induction motor drives, DTC seems to be particularly interesting being independent of machine rotor parameters and requiring no speed or position sensors. The DTC scheme is characterized by the absence of PI regulators, current regulators and PWM signals generators. The presence of hysteresis controllers for flux and torque could determine torque and current ripple and variable switching frequency operation for the voltage source inverter. To analyze DTC

principles, the strategies and the problems related to its implementation and the possible improvements have been discussed [7]. DTC technology [8] developed by ABB company in the mid of 1980's gives the fast torque response. The main difference between DTC and the traditional AC drive control methods is that with DTC there is no separate voltage and frequency-controlled PWM modulator.

A comparative study on two most popular control strategies for induction motor drives: Field-Oriented Control (FOC) and DTC have been presented. The comparison is based on various criteria including basic control characteristics, dynamic performance, parameter sensitivity, and implementation complexity [9]. Marcel et al [10] investigated direct and indirect vector control in both voltage and current controlled forms.

The fundamental relationship between the rotating speed of the stator flux linkage and torque is analysed and the design principle of controller is presented. Fixed switching frequency and low torque ripple are obtained with PI control and Space Vector Modulation (SVM) method [11]. A comprehensive comparison of the two main high performance induction machine torque control methods, FOC and DTC has been studied. A summary to the various techniques of torque ripple reduction followed by a proposed simple method to reduce the torque ripple is presented [12-13]. A DTC-SVM with PI and without PI controller direct torque control without hysteresis band has been compared. The average torque ripple is reduced over 60% with DTC-SVM with PI controller method compared with classical DTC [14]. DTC do not show good performance at low speed range with conventional open loop stator flux observer when stator resistance varied. Therefore, a new nonlinear stator flux observer in order to estimate the stator flux of induction motor at low speed has been shown with its simulation results. The simulation is carried out to the proposed controllers produce an excellent performance in minimizing the torque and stator flux ripples and maintaining a constant switching frequency [15-16]. The realization of variable voltage and variable frequency with two-stage controller converters and single stage PWM inverters is introduced. Reducing harmonics with multiple inverters or with one PWM inverter is discussed. Various control strategies for variable voltage, variable frequency drives are Volt/Hz, constant slip speed, and constant air gap flux controls. The limitation and merits of above control scheme and relevant modeling to evaluate their dynamic performance are developed [17].

A number of approaches to DTC-SVM are presented which combines ADRC (Auto Disturbance Rejection Ratio) and DTC-SVM principles within a simple and robust high performance drive. DTC used in AC-drive locomotive control system, which has been developed in the recent decade, is a control strategies with high dynamic and steady performance, and it directly generate the inverter gate control signal by sensing the output of the stator flux, torque hysteresis comparator and the position information of the stator flux that cause the variable switching frequency [18-22].

Lascu, Boldea and Blaabjerg [23] introduce a DTC-SVM for induction motor sensor less drives. It is able to reduce the acoustical noise, the torque, flux, current, and speed pulsations during steady state. This strategy realizes almost ripple-free operation for the entire speed range. Consequently, the flux, torque, and speed estimation is improved.

Direct vector control and indirect vector control are the two different types of control technique is applied, in which direct vector control method determines the magnitude and the position of the rotor flux vector by direct flux measurement. The flux is measured by the sensors like Hall Effect sensor, search coil and this is a part of the disadvantages. While, indirect vector control method, the motor speed is used as feedback signal in the controller and controller calculates the reference values of two decoupled components of stator current space vector in the synchronously rotating reference frame [24-29].

DTC control scheme for Induction Motor, which features in low torque ripple and low flux ripple by means of SVM with a simple, constant switching frequency and robust high performance drive has been presented. If the switching frequency could be fixed, the precious switching resources will be used fully and the cost of IGBT will be reduced greatly. DTC is widely used for ac drives and attempts to combine DTC with SVM have led to new ways [30-32].

A new method for DTC based on load angle control has been shown and use of simple equations to obtain the control algorithm makes it easy to understand and implement. Fixed switching frequency and low torque ripple are obtained using space vector modulation. This control strategy overcomes the most important drawbacks of classical DTC. Because of development of the power electronics in the branch of

frequency converters, the drives with variable speed with asynchronous motors required today a great interest. Technique for speed control of the induction motors is the SVM strategy, which allows the minimizing of the harmonics of current and torque [33-34].

A study has been carried out on duty ratio control scheme for inverter fed induction machines using the DTC method. An improved steady state torque response was achieved using the duty ratio control and had shown less torque ripple compared to the conventional DTC. Fuzzy logic control has been used to implement the duty ratio during each switching cycle using the torque and flux errors as inputs [35].

An effective space vector pulse width modulation (SVPWM) method for multi-level inverter fed induction motor is presented. This method is based on SVPWM method for two-level inverter. As the number of level increasing, the SVPWM method becomes more and more complex. An intrinsic relationship between multi-level and two-level is developed and by using a linear transformation, the switching time of vectors for two-level inverter can be transformed for multi-level inverter. A novel classification of voltage vectors is proposed to determine switching sequence. This method can be extended for N-level inverter [36-37].

A modified DTC-SVM for induction motor drives is proposed to minimize the torque ripple of induction motor in which, the stator flux level is selected in accordance with the efficiency optimized motor performance. The nonlinear controller has generated the reference of voltage space vector for a two level three phase SVM-PWM inverter, which feeds motor. Effects of sampling frequency, motor speed, and switching strategy on this current error are investigated and their effects on performance of the stator resistance PI compensator arc considered. The two different nonlinear observers one is Model Reference Adaptive System (MRAS) and another is Extended Kalman Filter (EKF) applied to sensorless DTC of IM, are discussed and compared to each other. The rotor speed estimation in DTC technique is affected by parameter variations especially the stator resistance due to temperature particularly at low speeds. Therefore, it is necessary to compensate this parameter variation in sensorless induction motor drives using an online adaptation of the control algorithm by the estimated stator resistance [38-56].

## 1.3 OBJECTIVE OF THE WORK

The objective of the present work is to obtain the reduced torque ripples, harmonics distortion with maintained constant switching frequency. DTC-SVM has been developed to improve the torque performance and to obtain the voltage space vector required to compensate the flux and torque errors.

## 1.4 ORGANIZATION OF THESIS

The work carried out has been summarized in five Chapters.

**CHAPTER 1** summarizes the overview of the problem, literature review, objectives of work and organization of the thesis.

**CHAPTER 2** presents the mathematical model of induction motor, its mathematical model in which voltage and flux equations are referred to synchronous reference frame and then converted into a stationary reference frame. The three phase equations is converted into the two phase equations by applying d-q model theory method (also called Park's Transformation). The information about the different control techniques of induction motor drives is presented.

**CHAPTER 3** deals the principle of conventional direct torque controlled induction motor drive, supplied by a voltage source inverter. The simulation results of current, speed, torque, stator flux linkage are shown for different conditions.

**CHAPTER 4** presents the DTC-SVM based induction motor drive. The SVM technique is discussed in detailed along the control strategy. The DTC-SVM model is simulated in MATLAB Simulink and the results are shown for different load torque and speed references.

**CHAPTER 5** summarize the main conclusions of the thesis work followed by suggestions for future work.

# CHAPTER 2

# MODELLING AND CONTROL TECHNIQUES OF INDUCTION MOTOR DRIVE

## 2.1 INTRODUCTION

Induction motors have been used in the past mainly in applications requiring a constant speed because conventional methods of their speed control have either been expensive or highly inefficient. Variable speed applications have been dominated by DC drives. Availability of thyristor, power transistors, IGBT (Insulated Gate Bipolar Transistor) and GTO (Gate Turn Off) have allowed the development of variable speed induction motor drives. The main drawback of DC motors is the presence of commutator and brushes, which require frequent maintenance and make them unsuitable for explosive and dirty environments. On the other hand, induction motors, particularly squirrel cage are rugged, cheaper, lighter, smaller, more efficient, require lower maintenance and can operate in dirty and explosive environments. Although variable speed induction motor drives are generally expensive than dc drives, they are used in a number of applications such as fans, blowers, cranes, conveyers, traction etc. because of the advantages of induction motors.

In the three-phase induction motors, stator carries a three-phase balanced distributed winding. When a three-phase supply completes one full cycle, the magnetic field of a two-pole motor has rotated through 360° in physical space. The motors with more pairs of poles require more power supply cycles to complete one physical revolution of the magnetic field and so these motors run slower. In Table 2.1 both DC Drives and DTC drives use actual motor parameters to control torque and speed. Thus, the dynamic performance is fast and easy. Also with DTC, for most applications, no tachometer or encoder is needed to feed back a speed or position signal. With PWM AC drives, the controlling variables are frequency and voltage which need to go through several stages before being applied to the motor. Thus, with PWM drives control is handled inside the electronic controller and not inside the motor.

Table 2.1 Comparison of control variables

| DRIVE | CONTROL VARIABLES |
|---|---|
| DC DRIVES | Armature Current, Field Current |
| AC DRIVES (PWM) | Voltage, Frequency |
| DIRECT TORQUE CONTROL | Motor Torque, Motor Magnetizing Flux |

### 2.1.1 d-q MODEL THEORY

In an adjustable speed drive, the machine normally constitutes an element within a feedback loop, and therefore its transient behavior has to be taken into consideration. Besides, high-performance drives control. Such as vector or field-oriented control, is based on dynamic d-q modal of the machine. Therefore, to understand vector control principal, a good understand of d-q modal is mandatory.

Basically, it can be looked on as a transformer with a moving secondary, where the coupling coefficient between the stator and rotor phase change continuously with the change of rotor position. The machine modal can be described by differential equation with time-varying mutual inductance, but such a modal tend to be very complex, note that a three phase machine can be represented by an equivalent two-phase machine in which $d_s$-$q_s$ correspond to stator direct and quadrature axes, and $d_r$-$q_r$ correspond to rotor direct and quadrature axes. Although it is somewhat simple, the problem of time-varying parameters still remains. R.H. Park in the 1920s, proposed a new theory of electrical machine analysis to solve this problem. The problem has been formulated with change of variable which, in effect, replaced the variable (voltage, current, and flux linkage) associated with the stator winding of a synchronous machine with variable associated with fictitious winding rotating with the rotor at synchronous speed. Then essentially, transformed, or referred the stator variable to a synchronously rotating reference frame fixed in the rotor. With such a transformation (called park's transformation), all the time varying inductances can be eliminated. Later, in the 1930s, H. C. Stanley showed that time-varying inductances in the voltage equation of an induction machine due to electric circuit in relative motion can be eliminated by transforming the rotor variable to variable

associated with fictitious stationary winding, in this case, the rotor variable are transformed to a stationary reference frame fixed on the stator. Later, G. Kron proposed a transformation of a both stator and rotor variable to a synchronously rotating reference frame that move with the rotating magnetic field. D.S. Brereton proposed a transformation of stator variables to a rotating reference frame that is fixed on rotor. In fact, it was shown later by Krause and Thomas that time-varying inductance can be eliminated by referring the stator and rotor variables to a common reference frame which may rotate at any speed (arbitrary reference frame). Without going deep into the rigor of machine analysis, it will try to develop a dynamic machine model in synchronously rotating and stationary reference frame.

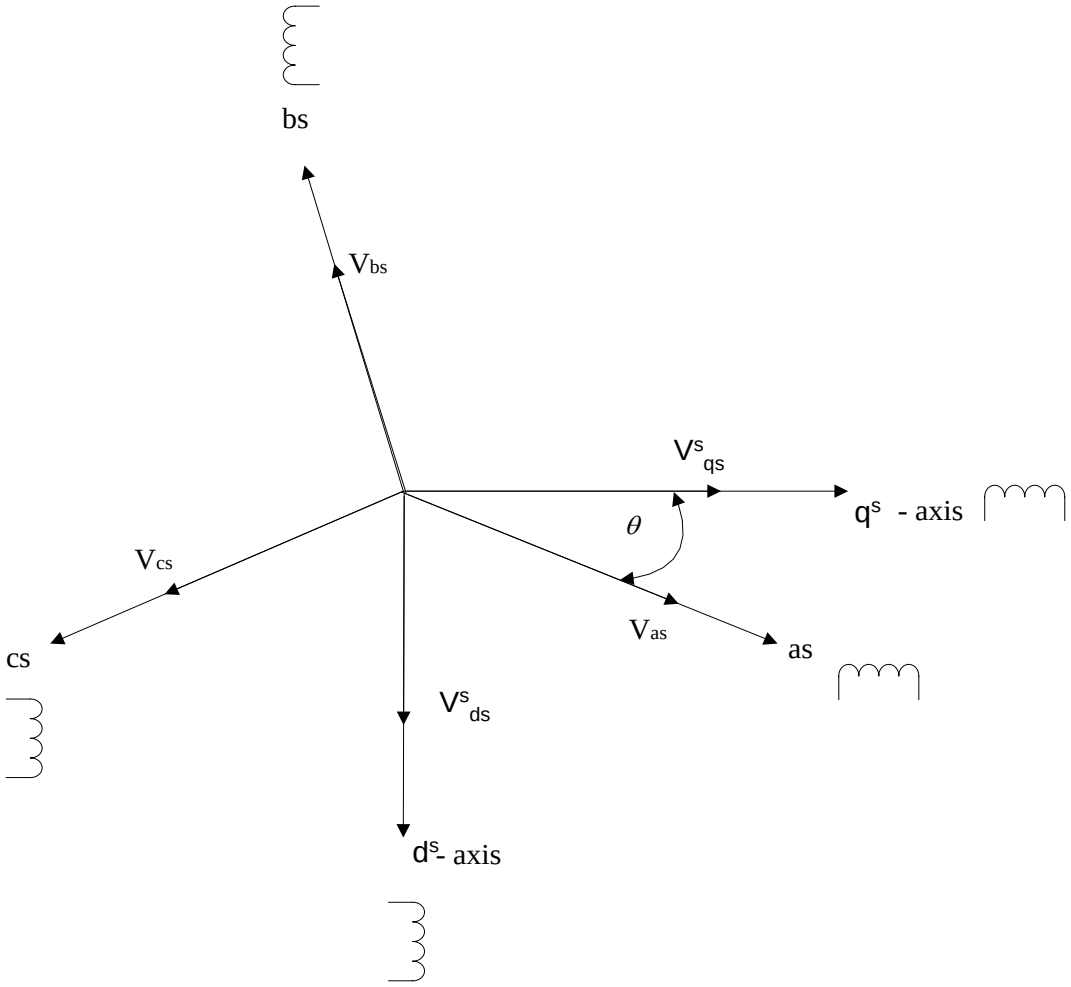


Fig.2.1 Stationary Frame a-b-c to $d^s$-$q^s$ Axes Transformation

### 2.1.1.1 *AXES TRANSFORMATION*

Consider a symmetrical three-phase induction machine with stationary $a_s$-$b_s$-$c_s$ axes at $2\pi/3$ angle apart, as shown in Figure 2.1. The main goal is to transform the three-phase stationary reference frame ($a_s$-$b_s$-$c_s$) variables into two phase stationary reference frame ($d^s$-$q^s$) variables and then transform these to synchronously rotating reference frame ($d^e$-$q^e$), and vice versa. Assume that the $d^s$-$q^s$ axes are oriented at 'θ' angle shown in Figure 2.1. The voltages $V_{ds}^s$ and $V_{qs}^s$ can be resolved into as-bs-cs components can be represented in the matrix form as:

$$\begin{bmatrix} V_{as} \\ V_{bs} \\ V_{cs} \end{bmatrix} = \begin{bmatrix} \cos\theta & \sin\theta & 1 \\ \cos(\theta - 120^0) & \sin(\theta - 120^0) & 1 \\ \cos(\theta + 120^0) & \sin(\theta + 120^0) & 1 \end{bmatrix} \begin{bmatrix} V_{qs}^s \\ V_{ds}^s \\ V_{os}^s \end{bmatrix} \tag{2.1}$$

The corresponding inverse relation is:

$$\begin{bmatrix} V_{qs}^s \\ V_{ds}^s \\ V_{os}^s \end{bmatrix} = \frac{2}{3} \begin{bmatrix} \cos\theta & \cos(\theta - 120^0) & \cos(\theta + 120^0) \\ \sin\theta & \sin(\theta - 120^0) & \sin(\theta + 120^0) \\ 0.5 & 0.5 & 0.5 \end{bmatrix} \begin{bmatrix} V_{as} \\ V_{bs} \\ V_{cs} \end{bmatrix} \tag{2.2}$$

Where, $V_{os}^s$ is added as the zero sequence component, which may or may not be present. The voltage has been considered as the variable. The current and flux linkage can be transformed by similar equations. It is convenient to set θ = 0, so that the $q^s$-axis is aligned with the as-axis. Ignoring the zero sequence components, the transformation relations can be simplified with the help of equations (2.1) and (2.2) by assuming $\theta$ = 0 in these respective equations as:

$$V_{as} = V_{as} \tag{2.3}$$

$$V_{bs} = -\frac{1}{2} V_{qs}^s - \frac{\sqrt{3}}{2} V_{ds}^s \tag{2.4}$$

$$V_{cs} = -\frac{1}{2} V_{qs}^s + \frac{\sqrt{3}}{2} V_{ds}^s \tag{2.5}$$

and inverse equations are expressed as:

$$V_{qs}^{s} = \frac{2}{3} V_{as} - \frac{1}{3} V_{bs} - \frac{1}{3} V_{cs} = V_{as} \quad (2.6)$$

$$V_{ds}^{s} = -\frac{1}{\sqrt{3}} V_{bs} + \frac{1}{\sqrt{3}} V_{cs} \quad (2.7)$$

### 2.1.2 MATHEMATICAL MODEL OF INDUCTION MOTOR

An induction motor is modeled using voltage and flux equations which are referred to synchronous reference frame, denoted by the superscript "e".

**Stator Voltage Equation:**

$$V_s^e = R_s\, i_s^e + j\omega_e\, \lambda_s^e + p\, \lambda_s^e \quad (2.8)$$

**Rotor Voltage Equation:**

$$0 = R_r\, i_r^e + j(\omega_e - \omega_r)\, \lambda_r^e + p\, \lambda_r^e \quad (2.9)$$

**Stator Flux Equation:**

$$\lambda_s^e = L_s\, i_s^e + L_m\, i_r^e \quad (2.10)$$

**Rotor Flux Equation:**

$$\lambda_r^e = L_r\, i_r^e + L_m\, i_s^e \quad (2.11)$$

**Mechanical Equation:**

$$T_e - T_L = J_m\, p\, \omega_r + B_m\, \omega_r \quad (2.12)$$

$$T_e = \frac{3P}{2} ( \lambda_{sd}^e\, i_{sq}^e - \lambda_{sq}^e\, i_{sd}^e ) \quad (2.13)$$

By referring to a stationary reference frame, denoted by the superscript "s", with d-axis attached on the stator winding of phase "A", the mathematical equations of induction motor can be rewritten as follows.

**Stator Voltage Equation:**

$$V_s^s = R_s\, i_s^s + p\, \lambda_s^s \quad (2.14)$$

**Rotor Voltage Equation:**

$$0 = R_r\, i_r^s - j\omega_r\, \lambda_r^s + p\, \lambda_r^s \quad (2.15)$$

**Stator Flux Equation:**

$$\lambda_s^s = L_s\, i_s^s + L_m\, i_r^s \quad (2.16)$$

**Rotor Flux Equation:**

$$\lambda_r^s = L_r\, i_r^s + L_m\, i_s^s \tag{2.17}$$

**Mechanical Equation:**

$$T_e = \frac{3P}{2}\frac{L_m}{\sigma L_s L_r}\left(\lambda_{sd}^s\, i_{rq}^s - \lambda_{sq}^s\, i_{rd}^s\right) \tag{2.18}$$

$$T_e - T_L = J_m\, p\, \omega_r + B_m\, \omega_r \tag{2.19}$$

Where, $\sigma$ = total leakage factor,

$$\sigma = 1 - \frac{L_m^2}{L_s L_r} \tag{2.20}$$

All of the above equations explain, the modeling of induction motor in synchronous reference frame and stationary reference frame.

## 2.2 DIFFERENT CONTROL TECHNIQUES OF INDUCTION MOTOR (IM) DRIVES

There are mainly three main control techniques of induction motor drive:

1) Scalar Control Technique (V/f Control).
2) Vector Control Technique or Field Oriented (FO) Technique.
3) Direct Torque Control (DTC) Technique.

### 2.2.1 SCALAR CONTROL TECHNIQUE

Scalar Control (V/f Control) is one common speed control technique for variable frequency drives (VFDs, frequency changers, frequency inverters) in the industry. In this type of control, the motor is fed with variable frequency signals generated by the Pulse Width Modulation (PWM) control from an inverter. Here, the V/f ratio is maintained constant in order to get constant torque over the entire operating range. Since only magnitudes of the input variables (frequency and voltage) are controlled, this is known as "scalar control". Generally, the drives with such a control are without any feedback devices (open-loop control). Hence, a control of this type offers low cost and is an easy to implement solution.

In such controls, very little knowledge of the motor is required for frequency control. So, scalar control is widely used. A disadvantage of scalar control is that the torque developed is load dependent, as it is not controlled directly. Also, the transient response of such a control is not fast due to the predefined switching pattern of the inverter. However, if there is a continuous block to the rotor rotation, it will lead to heating of the motor regardless of implementation of the over-current control loop. By adding a speed/position sensor, the problem relating to the blocked rotor and the load dependent speed can be overcome. However, this will add to the system cost, size and complexity.

### 2.2.2 VECTOR CONTROL TECHNIQUE OR FIELD ORIENTED (FO) TECHNIQUE

The Field Oriented Control (FOC) is by far the most widely accepted method of control in high performance ac drive domains. While FOC represents a single, unified control concept, the application strategies, complexity of implementation and drive responses vary with different drive motors. The principle behind the field oriented control or the vector control is that the machine flux and torque are controlled independently, in a similar fashion to a separately excited DC machine. The vector control technique decouples the two components of stator current space vector: one providing the control of flux and the other providing the control of torque.

An induction motor is said to be in vector control mode, if the decoupled components of the stator current space vector and the reference decoupled components defined by the vector controller in the synchronously rotating frame match each other respectively. FOC technique operates the induction motor like a separately excitedly DC motor and vector control further classified into direct vector control and indirect vector control.

### 2.2.3 DIRECT TORQUE CONTROL (DTC) TECHNIQUE

In addition to vector control systems, instantaneous torque control yielding very fast torque response can be obtained by employing DTC. Drives with direct torque control DTC are finding great interest, since in the mid of 1980's, 'ABB' introduced the first industrial direct-torque-controlled induction motor drive. In a DTC drive, flux linkage and electromagnetic torque are controlled directly and independently by the selection of optimum inverter switching modes. The selection is made to restrict the flux linkage and electromagnetic torque errors within the respective flux and torque hysteresis bands, to obtain fast torque response, low inverter switching frequency and low harmonic losses. The required optimal switching voltage vectors can be selected by using a so called optimum switching voltage vector look-up table. This can be obtained by simple physical considerations involving the position of the stator flux linkage space vector, the available switching vectors and the required torque and flux linkage.

## 2.3 CONCLUDING REMARKS

Induction motor is the best choice for loads requiring low starting torques and substantially constant speeds because of its ruggedness, simplicity, low cost and reduced maintenance charges. In the modelling of the induction motor, the three phase stator equations are then converted into two phase equations in stationary reference frame by d-q model theory. There are three different control techniques of induction motor drives namely Scalar Control technique, Vector Control technique and DTC, among all of three techniques, DTC technique gives fast torque response as well as better control over torque and flux, also it doesn't require any coordinate transformation between stationary frame and synchronous frame in comparison with conventional vector controlled drives.

# CHAPTER 3
# CONVENTIONAL DIRECT TORQUE CONTROL (DTC)

## 3.1 INTRODUCTION

Using Direct Torque Control (DTC) or Direct Self Control (DSC), it is possible to obtain a good dynamic control of the torque without any mechanical transducer on the machine shaft. Thus DTC and DSC can be considered as "sensor less type" control techniques. The DSC is preferable in the high power range applications where a lower inverter switching frequency can justify higher current distortion. The basic concept of direct torque control induction motor drives is to control both stator flux and electromagnetic torque of the machine independently. The DTC based drives do not require the coordinate transformation between stationary frame and synchronous frame in comparison with the conventional vector controlled drives. The name DTC is derived by the fact that on the basis of the error between the reference and the estimated values of the torque and flux, it is possible to directly control the inverter states in order to reduce the torque and flux error within limits. DTC uses an induction motor model to predict the voltage required to achieve a desired output torque. By using only current and voltage measurements, it is possible to estimate the instantaneous stator flux and output torque. An induction motor model is then used to predict the voltage requirement to drive flux and torque to the demanded value with in a fixed time period.

Voltage source inverter fed induction motors are increasingly being used in general applications by varying the input voltage to the motor with frequency on open loop, is one of the popular methods of speed control. In this method V/f is held constant. In steady state operation, the machine air gap flux is approximately related to V/f. As the frequency approaches zero near zero speed, the magnitude of the stator voltage also tends to zero and this low voltage is absorbed by the stator resistance. Therefore, at low speed of operation the stator resistance drop is compensated by injecting an auxiliary voltage so that rated air gap flux and full load torque becomes available up to almost zero speed. At steady state operation, if the load torque is increased, the slip will increase within the

stability limit and a balance will be maintained between the developed torque and the load torque. However, if the voltage to the inverter fluctuates, the air gap flux will vary. Furthermore, increase in the stator resistance due to temperature results in the variation of air gap flux. Hence, the air gap flux may drift and as a result the torque sensitivity with slip frequency (or stator current) will vary. If the V/f ratio is not maintained, the flux may weak (or saturate) and in the constant V/f control scheme if the air gap flux decreases, slip frequency ($\omega * s$) will increase for the same torque demand, resulting into detoriation of machine response. Hence, a control scheme with independent control of torque and flux loop is desirable. DTC is one such scheme of speed control. Conventional AC drives are not capable to provide a fast and smooth variation in speed, required for servo drive applications in small scale packaging industry etc.

The idea of torque control in DTC or DSC scheme is to increase the torque angle (angle between stator flux and rotor flux) in case torque output needs to be increased. But the stator linked flux is kept intact at the desired magnitude. The change in the torque angle is performed by acceleration or deceleration of the angular speed of the stator linked flux vector, by application of the suitable voltage vector using voltage source inverter. The flux linking to rotor changes simultaneously with the change in stator flux. But a time lag appears between the changing rotor flux and change in the rotor current, due to rotor circuit time constant. Thus the rotor flux, which is proportional to the rotor current, does not change as fast as the stator flux.

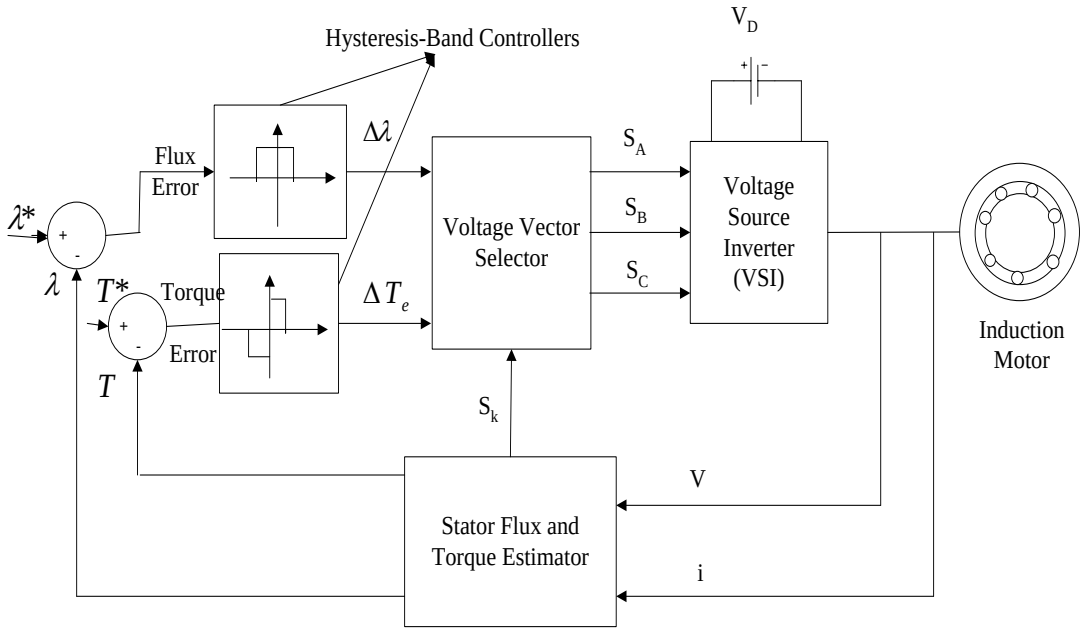


Fig.3.1 Conventional DTC Drive Configuration

Thus the torque angle can be increased or decreased with acceleration and deceleration of the rotating stator linked flux vector and control is achieved over the developed torque by the motor. In the Figure 3.1, Configuration of Conventional DTC drive is shown, in which the comparison between the reference and the actual value is taken and the errors are processed through hysteresis band controllers. The flux loop controller has two levels of digital output and the torque control loop has three levels of digital output. The feedback flux and torque are calculated from the induction machine terminal voltages and currents. The three phase terminals quantities are converted into two phase stationary d-q components, which are used for estimating motor torque and stator linked flux. Based on the resultant flux position and the errors in flux magnitude and in torque, a three-dimensional look up table is referred to decide the inverter switching. The 'Stator Flux and Torque Estimator' block shown in Figure 3.1 gives the sector number $S_k$ (in which the flux vector $\lambda$ lies) which is fed to the 'Voltage Vector Selector' block.

### 3.1.1 MAIN FEATURES OF DTC TECHNOLOGY

- Direct Control of flux and torque.
- Indirect control of stator currents and voltages.
- Stator fluxes are approximately sinusoidal.
- Reduced torque oscillations.
- Fast dynamic performances.

### 3.1.2 ADVANTAGES OF DTC

- Only the sector where the flux linkage space vector is located has to be determined.
- Minimize torque response time.

### 3.1.3 DISADVANTAGES OF DTC

- Inherent torque and stator flux ripple.
- Requirement of torque and flux estimators, implying the consequent parameters identification.

## 3.2 DTC PRINCIPLE

The electromagnetic torque in the three phase induction machine can be expressed as:

$$T_e = \frac{3}{2} P \left( \overrightarrow{\lambda_s^s} \times \overrightarrow{i_s^s} \right) \quad (3.1)$$

Where, $\overrightarrow{\lambda_s^s}$ = Stator Flux Linkage Space Vector, $\overrightarrow{i_s^s}$= Stator Current Space Vector

Both fixed to the stationary reference frame fixed to the stator and 'P' is the number of pairs of poles.

$\overrightarrow{\lambda_s^s}$ can be expressed as, $\overrightarrow{\lambda_s^s} = |\lambda_s^s| \, e^{j\rho_s}$.

Where, $\rho_s$ is the angle of the stator flux linkage space vector with respect to the d-axis of the stator reference frame shown in Figure 3.2

And, $\overrightarrow{i_s^s}$ can be expressed as, $\overrightarrow{i_s^s} = |i_s^s| \, e^{j\Phi_s}$

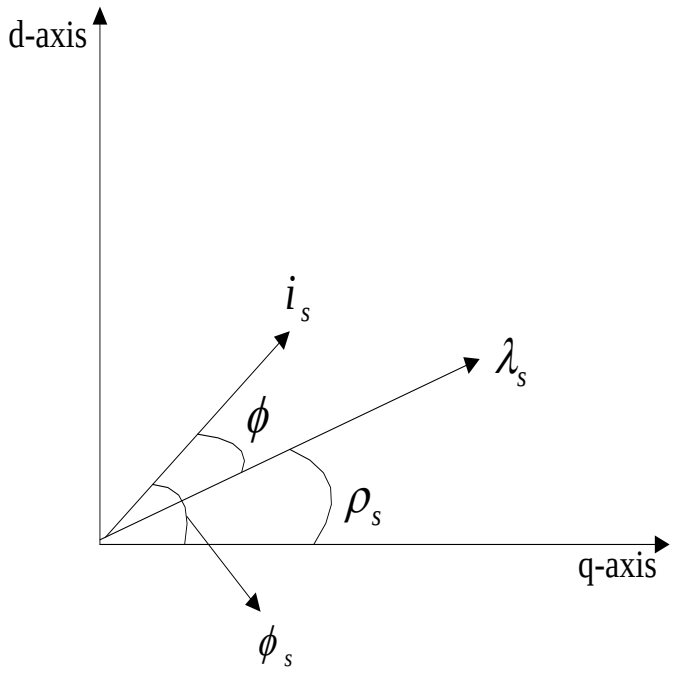


Fig.3.2 Stator Flux-Linkage and Stator Current Space Vectors

Equation (3.1) can be expressed as follows:

$$T_e = \frac{3}{2} p \, |\overrightarrow{\lambda_s^s}| \, |\overrightarrow{i_s^s}| \sin(\phi_s - \rho_s) \tag{3.2}$$

$\rho_s$ is the stator flux angle and $\phi_s$ is the stator current in the stationary frame. It can be shown by using the voltage equations of the induction machine that, for a given value of the rotor speed, if the stator flux linkage space vector is kept constant and the angle $\rho_s$ is changed, then the electromagnetic torque can be rapidly changed.

### 3.2.1 MATHEMATICAL PRESENTATION

In stationary reference frame, the rotor current space vector can be expressed in terms of the stator flux linkage space vector and is given by:

$$\overrightarrow{i_s^s} = \frac{\left(\overrightarrow{\lambda_s^s} - L_s \overrightarrow{i_s^s}\right)}{L_m} \tag{3.3}$$

By using equations:

$$\overrightarrow{\lambda_r^s} = L_r \overrightarrow{i_s^s} + L_m \overrightarrow{i_s^s} \tag{3.4}$$

and equation (3.3) the rotor flux linkage space vector can be expressed as:

$$\overrightarrow{\lambda_r^s} = \frac{L_r}{L_m} \left(\overrightarrow{\lambda_s^s} - L_s \overrightarrow{i_s^s}\right) \tag{3.5}$$

Now, by substituting above two equations in rotor voltage equation expressed in stationary reference frame$\left(i.e.\ 0 = R_r \vec{i_s^s} + \frac{d}{dt} \vec{\lambda_r^s} - j\omega_r \vec{\lambda_r^s}\right)$, we can express the rotor voltage equation in terms of $\vec{i_s^s}$ and $\vec{\lambda_s^s}$.

This can be used to express the stator current space vector in terms of the stator flux linkage space vector. This expression for the stator current space vector is then substituted in equation 3.1 and from that we can see that the electromagnetic torque depends upon stator flux linkage space vector and the angle of the stator flux linkage space vector with respect to the direct axis of the stator reference frame, $\rho_s$ .Thus by forcing the largest $d\rho_s/dt$ under the condition of constant stator flux linkage, the fastest electromagnetic torque response time is obtained. In other words, if such stator voltages are imposed on the motor, which keep the stator flux constant (at the demanded value), but which quickly rotate the stator flux-linkage space vector into the position required (by the torque demand), then fast torque control is performed.

So, the electromagnetic torque can be quickly changed by controlling the stator flux linkage space vector, which however can be changed by using appropriate stator voltages generated by the inverter which supplies the induction motor. It can be seen that direct stator flux and electromagnetic torque control is achieved by using the appropriate stator voltages. This type of control is usually referred to as direct torque control.

## 3.3 LOOK UP TABLE SELECTION

The required stator flux is maintained by means of choosing the most suitable VSI state. If the ohmic drop is neglected, then the stator voltage impresses directly the stator flux in accordance with the equation given as:

$$\frac{d}{dt} \vec{\lambda_s} = \vec{V_s} \text{ or } \Delta\lambda_s = \vec{V_s}\,\Delta t \qquad (3.6)$$

Decoupled control of the stator flux and torque is achieved by using radial and tangential components of the stator flux linkage space vector in its locus. These two components are directly proportional to the components of the same voltage space vector in the same directions. Figure 3.3 shows the possible dynamic locus of the stator flux, and its variation depending on the chosen VSI states. The possible global locus is divided into six different sectors shown by the discontinuous line. From Figure 3.3, the general table

can be framed. It can be seen from the Table 3.1 that the states $V_k$ and $V_{k+3}$, are not considered in the torque because they can both increase (initial $30^0$ degrees) or decrease (next $30^0$ degrees) the torque at the same sector depending on the stator flux position.

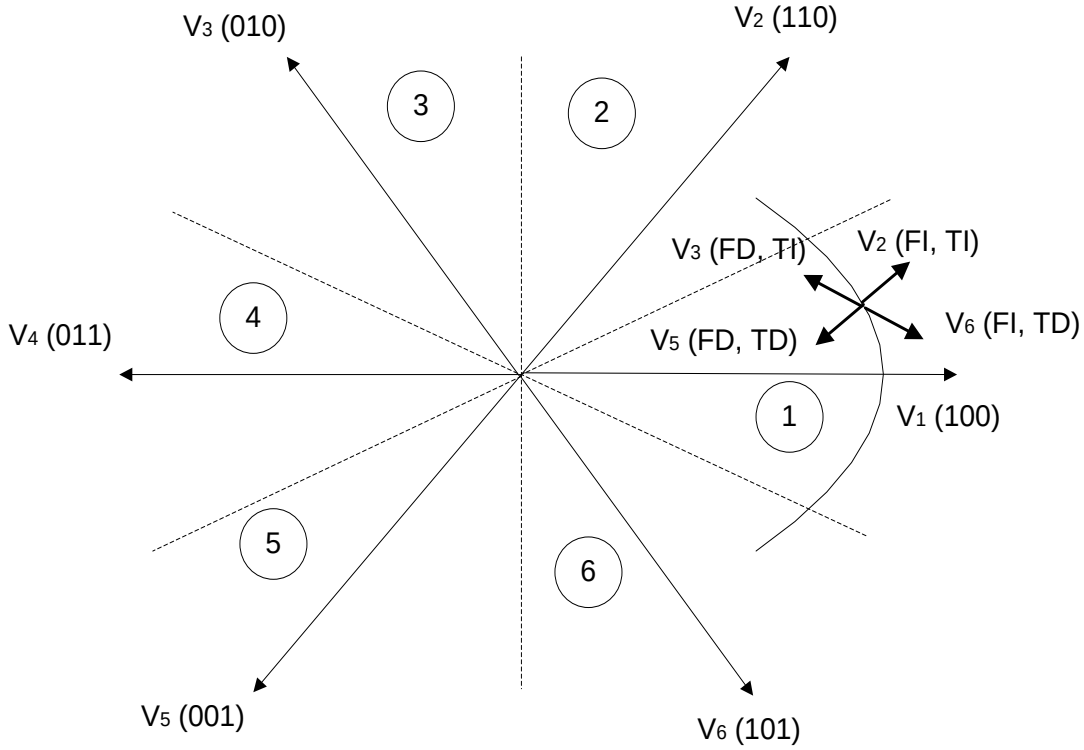


Fig.3.3 Stator Flux Vector Locus and Different Possible Switching Voltage Vectors. FD: Flux Decreases, FI: Flux Increases TD: Torque decreases, TI: Torque Increases.

Table 3.1: General Selection Table of DTC for $k^{th}$ the Sector Number.

| Voltage Vector | Increase | Decrease |
|---|---|---|
| Stator Flux | $V_k$ , $V_{k+1}$ , $V_{k-1}$ | $V_k$ , $V_{k-2}$ , $V_{k+3}$ |
| Torque | $V_{k+1}$ , $V_{k+2}$ | $V_{k-1}$ , $V_{k-2}$ |

Finally, The DTC classical table is as follows:

Table 3.2: Switching Vector Selection Table

| λ | T | $S_1$ | $S_2$ | $S_3$ | $S_4$ | $S_5$ | $S_6$ |
|---|---|---|---|---|---|---|---|
| FI | TI | $V_2$ | $V_3$ | $V_4$ | $V_5$ | $V_6$ | $V_1$ |
| | TE | $V_0$ | $V_7$ | $V_0$ | $V_7$ | $V_0$ | $V_7$ |
| | TD | $V_6$ | $V_1$ | $V_2$ | $V_3$ | $V_4$ | $V_5$ |
| FD | TI | $V_3$ | $V_4$ | $V_5$ | $V_6$ | $V_1$ | $V_2$ |
| | TE | $V_7$ | $V_0$ | $V_7$ | $V_0$ | $V_7$ | $V_0$ |
| | TD | $V_5$ | $V_6$ | $V_1$ | $V_2$ | $V_3$ | $V_4$ |

FD/FI: Flux decreases/Increases.

TD/TE/TI: Torque decreases/equal/Increases.

Where,

$S_k$: Stator flux sector.

$\lambda$: Stator flux modulus error after the hysteresis block.

T: Torque error after hysteresis block.

The sectors of the stator flux space vector are denoted from $S_1$ to $S_6$. Stator flux error after the hysteresis block can take three values. The zero voltage vectors $V_0$ and $V_7$ are selected when the torque error is within the given hysteresis limits, and must remain unchanged.

## 3.4 CONVENTIONAL DTC STRATEGY

As it can be seen, in the given Figure 3.4 there are two different loops, one for stator flux and other for torque. The reference values for the stator flux and the torque are compared with the corresponding actual values, and error is fed into the two level and three level hysteresis blocks respectively. The output of the hysteresis block, together with the position of the stator flux (divided into six different sectors) are fed into the

selection table/lookup table which gives appropriate switching vector to the inverter. In accordance with Figure 3.3, the stator flux modulus and torque errors tend to be restricted within its respective hysteresis bands.

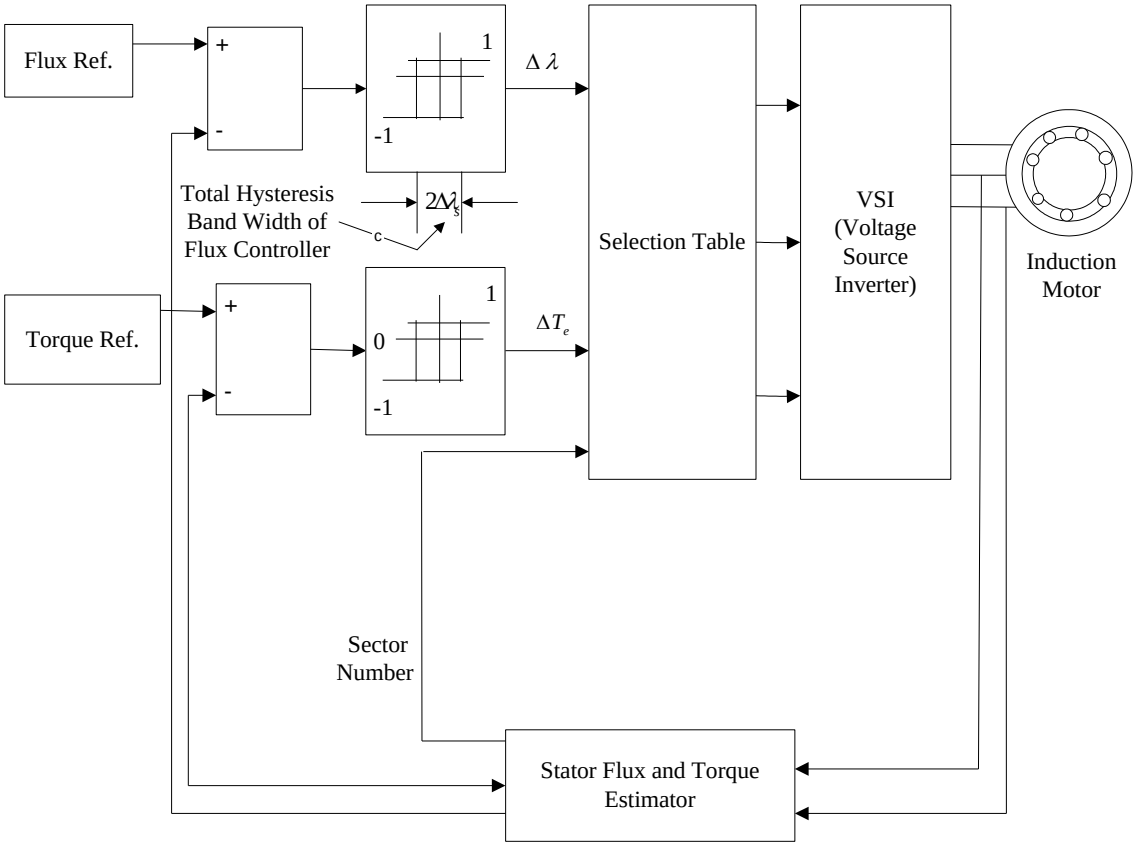


Fig.3.4 Direct Torque Control Schematic

The DTC requires the flux and torque estimations, which can be obtained as it is shown proposed in Figure 3.4, by using of two different phase currents, state of the inverter and mechanical speed or shaft position. However, flux and torque estimations can be performed using other parameters such as two stator currents and the mechanical speed, or two stator currents again and the shaft position. The DTC control scheme of the stator flux based DTC induction motor drive with VSI is shown in Figure 3.3. The scheme is composed of flux comparator, torque comparator, inverter optimum switching table, electromagnetic torque and stator flux linkage estimator and voltage source inverter.

### 3.4.1 FLUX AND TORQUE COMPARATORS

In Figure 3.4, the reference value of the stator flux linkage space vector is compared with the actual value of stator flux linkage space vector and the error is fed into the two level stator flux hysteresis comparator. Similarly, the reference value of the electromagnetic torque is compared with the actual value of electromagnetic torque and the torque error is fed into the three level torque hysteresis comparator

### 3.4.2 VOLTAGE SOURCE INVERTER

The VSI is a six-pulse self commutated inverter. The VSI is getting control pulses from the inverter optimal switching table. The stator flux-linkage space vector is:

$$\lambda_s = \int (V_s - R_s i_s)\, dt \qquad (3.7)$$

From equation (3.7), if the stator ohmic drop is neglected, then equation (3.7) can be modified as:

$$\frac{d\lambda_s}{dt} = V_s \qquad (3.8)$$

From the equation (3.8) we get $\Delta\lambda_s = V_s \Delta t$. So in a short, $\Delta t$ time, when the voltage vector is applied, $\Delta\lambda_s = V_s \Delta t$ that means the stator flux linkages move by $\Delta\lambda_s$ in the direction of stator voltage space vector at a speed which is proportional to the magnitude of the stator voltage space vector which is proportional to the DC voltage. By considering the six-pulse VSI shown in Figure 3.5, there are six non zero active voltage switching space vectors ($V_1, V_2 \ldots\ldots V_6$) and two zero space vectors ($V_0$ and $V_7$).These are shown in Figure 3.6. The six active inverter switching vectors can be expressed as:

$$V_s = V_k = \frac{2}{3} V_D\, e^{j(k-1)\frac{\pi}{3}} \quad , k = 1,2\ldots\ldots\ldots\ldots\ldots..6 \qquad (3.9)$$

Where, $V_D$ is the DC link voltage. For k = 7,8, $V_k = 0$ holds for the two zero switching states where the stator windings are short circuited, $V_s = V_k = 0$

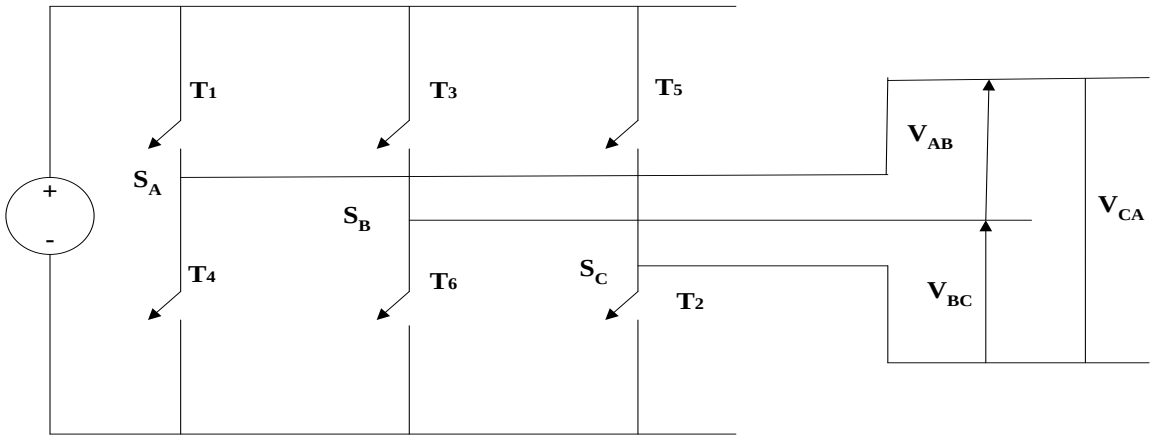


Fig.3.5 Six Pulse Voltage Source Inverter

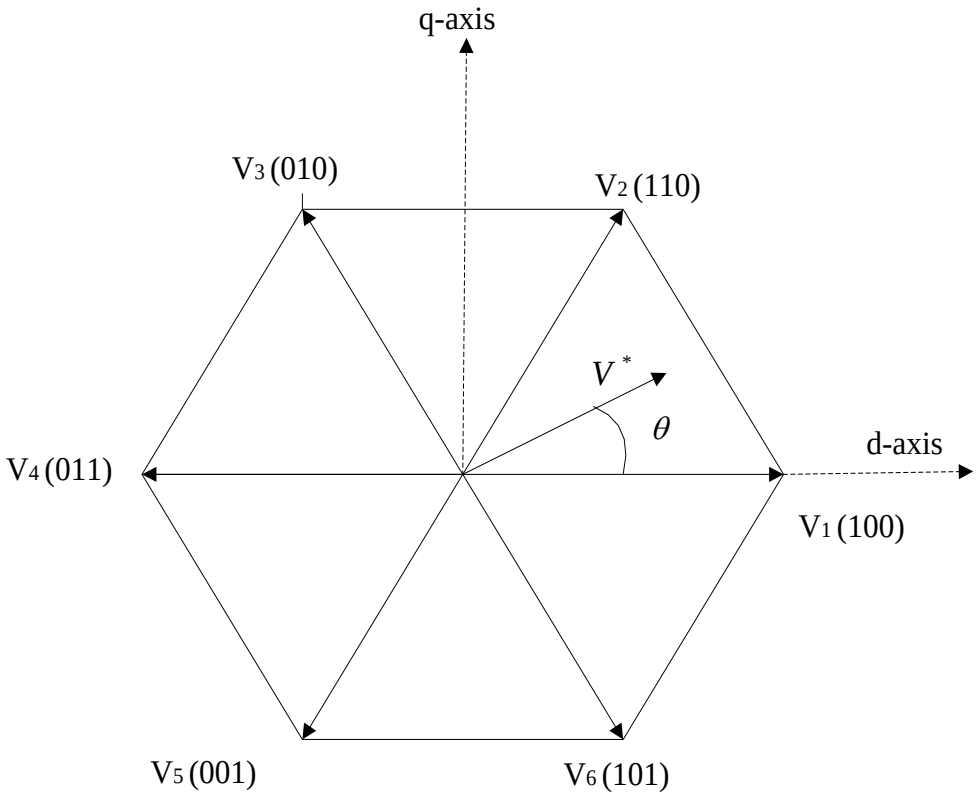


Fig.3.6 Space Vector Diagram

### 3.4.3 STATOR FLUX-LINKAGE SPACE VECTOR CONTROL

From the equation 3.6, the stator flux linkage space vector will change position move fast if non-zero switching vector are applied; and for a zero vector, it will not change (it will move very slowly due to the small ohmic voltage drop). In the DTC drive, at every sampling period, the switching vector is selected such that the stator flux-linkage error and torque errors should be confined within the respective hysteresis band. The drive may lose the control, if the width of the hysteresis bands is too small value. It is assumed that the total hysteresis band width of flux controller is $2\Delta\lambda_s$. If the selected switching vector is zero, then the speed of the stator flux-linkage space vector is zero, which can be change by changing the output ratio between the zero and non-zero voltage vectors and the duration of the zero states has a direct effect on the electromagnetic torque oscillation. If a reduced stator flux linkage space vector is required, it can be achieved by applying switching voltage vector, which is shown in Figure 3.7. The stator flux linkage space vector $\lambda_s$ within the hysteresis band, whose total band width is $2\Delta\lambda_s$ as shown in Figure 3.7. The locus of the flux linkage space vector is divided in to several sectors, and due to the six step inverter, the minimum number of sectors required is six. The sectors are also shown in Figure 3.7 as dotted line. There are eight switching vectors to keep the modulus of the stator flux linkage space vector $\lambda_s$ within the hysteresis band. It is assumed that initially the stator flux linkage space vector is at position $P_0$, thus in sector 1. Assuming that the stator flux linkage space vector is rotating in anticlockwise, from Figure 3.7, by observing the stator flux linkage space vector at position $P_0$, it is at the upper limit $|\lambda_s| + \Delta\lambda_s$ so it must be reduced. This can be achieved by applying the suitable switching vector $V_3$, as shown in Figure 3.7. Thus, the stator flux linkage space vector will move rapidly from position $P_0$ to $P_1$ which is sector 2. At point $P_1$ the stator flux linkage space vector is again at its upper limit, it has to be reduced when it is rotated in anticlockwise, hence for this purpose the switching vector $V_4$ has to be selected, and then $\lambda_s$ moves from point $P_1$ to point $P_2$ as shown in Figure 3.7.

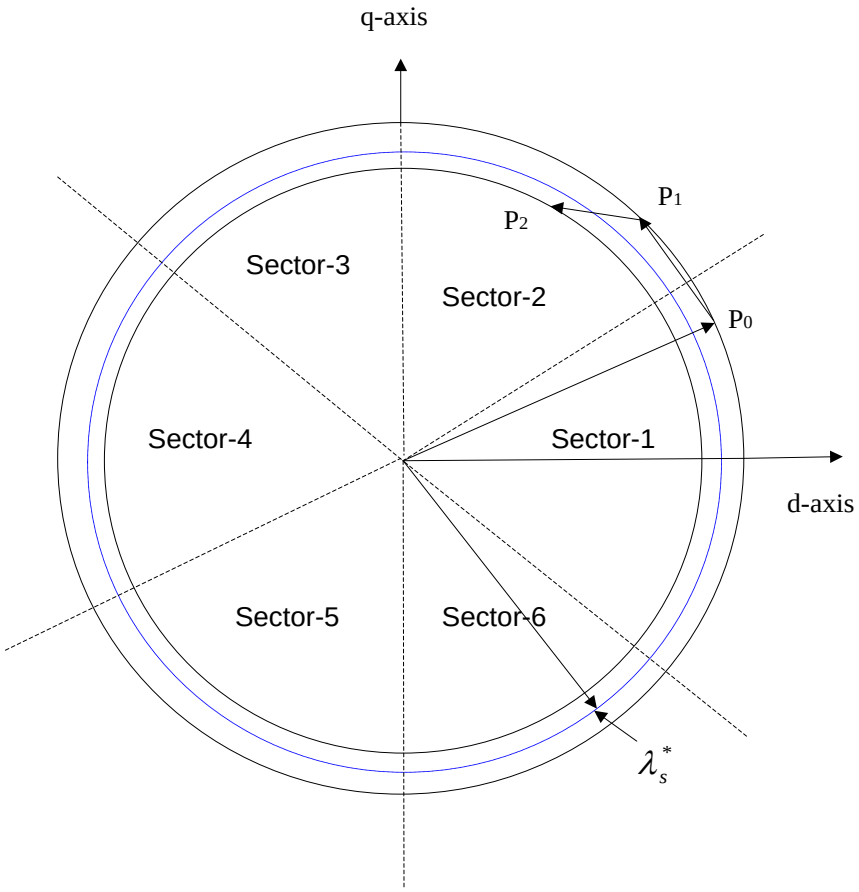


Fig.3.7 Stator Flux linkage Space Vector Locus

On the other hand, if the stator flux-linkage space vector moves in the clockwise direction from point $P_0$, then switching vector $V_5$ would have to be selected, since this would ensure the required rotation and also the required flux decreases. On the other hand, if at point $P_1$ the rotation of the stator flux-linkage space vector has to be stopped, then a zero switching vector would have to be applied.

If an increase of the torque is required, then the torque is controlled by applying voltage vectors that advance the flux linkage space vector in the direction of rotation and if a decrease is required, voltage vectors are applied which oppose the direction of the torque and if zero torque is required then zero switching vector is applied which minimizes the inverter switching. It follows that the angle of the stator voltage space vector is indirectly controlled through the flux vector and torque, and increasing torque causes an increased torque angle.

### 3.4.4 OPTIMAL SWITCHING TABLE OF INVERTER

The outputs of the two comparators ($\Delta\lambda$ , $\Delta T_e$) are used in the inverter optimal switching table (look-up-table), which also uses the information on the position of the stator flux-linkage space vector. The Table 3.2 is known as optimum switching vector selection table. This gives the optimum selection of the switching vectors for all the possible stator flux-linkage vector positions.

The digital output signal of a two level flux hysteresis comparator is

$\Delta\lambda = 1$ if $|\lambda_s| \leq (|\lambda_s^*| - \Delta\lambda_s)$, Stator flux to be increased.

$\Delta\lambda = 0$ if $|\lambda_s| \geq (|\lambda_s^*| - \Delta\lambda_s)$, Stator flux to be decreased.

The digital output signals of a three level flux hysteresis comparator are:

When the stator flux-linkage space vector rotates in the forward direction (anticlockwise direction)

$dT_e = 1$ if $|T_e| \leq (|T_e^*| - |\Delta T_e|)$, Torque to be increased.

$dT_e = 0$ if $|T_e| \geq |T_e^*|$, No change in torque is required.

For the stator flux-linkage space vector rotates in the forward direction (clockwise direction)

$dT_e = -1$ if $|T_e| \leq (|T_e^*| + |\Delta T_e|)$, Torque to be decreased.

$dT_e = 0$ if $|T_e| \leq |T_e^*|$, No change in torque required.

### 3.4.5 ESTIMATION OF STATOR FLUX LINKAGE SPACE VECTOR POSITION

The position of the stator flux linkage space vector (stator flux angle $\rho_s$) can be determined by using the estimated values of the direct and quadrature axis stator flux-linkages in the stationary reference frame$(\lambda_{sd},\ \lambda_{sq})$, thus the stator flux angle $\rho_s$ is:

$$\rho_s = \tan^{-1}\left(\frac{\lambda_{sq}}{\lambda_{sd}}\right) \qquad (3.10)$$

### 3.4.6 ESTIMATION OF ELECTROMAGNETIC TORQUE AND STATOR FLUX LINKAGE

The stator flux linkage space vector is:

$$\lambda_s = \int \left( V_{sq} - R_s i_{sq} \right) dt \tag{3.11}$$

Where, $\lambda_s = \lambda_{sd} + j\lambda_{sq}$ , $V_s = V_{sd} + jV_{sq}$ and $i_s = i_{sd} + ji_{sq}$

$$\lambda_{sd} = \int ( V_{sd} - R_s i_{sd}) dt \tag{3.12}$$

$$\lambda_{sq} = \int \left( V_{sq} - R_s i_{sq} \right) dt \tag{3.13}$$

Where, $\lambda_{sd}$, $V_{sd}$, $i_{sd}$ and $\lambda_{sq}$, $V_{sq}$, $i_{sq}$ are the d-axis and q-axis quantities of stator flux linkage space vector, stator voltage space vector and stator current space vector component respectively.

The electromagnetic torque is given by:

$$T_e = \frac{3}{2} P \left( \lambda_{sd} i_{sq} - \lambda_{sq} i_{sd} \right) \tag{3.14}$$

## 3.5 SIMULATION MODEL OF CONVENTIONAL DTC

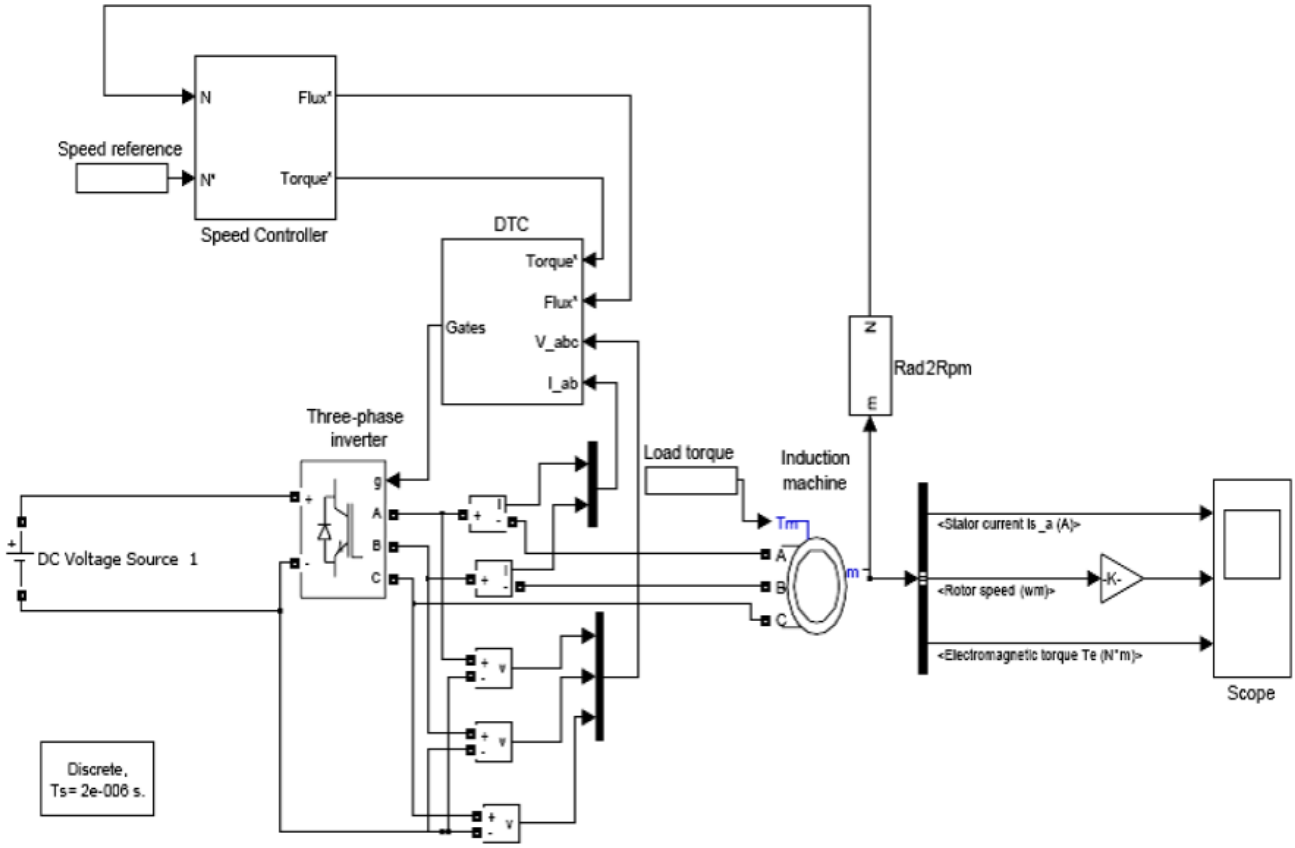


Fig.3.8(a) Simulation Model of Conventional DTC Induction Motor Drive

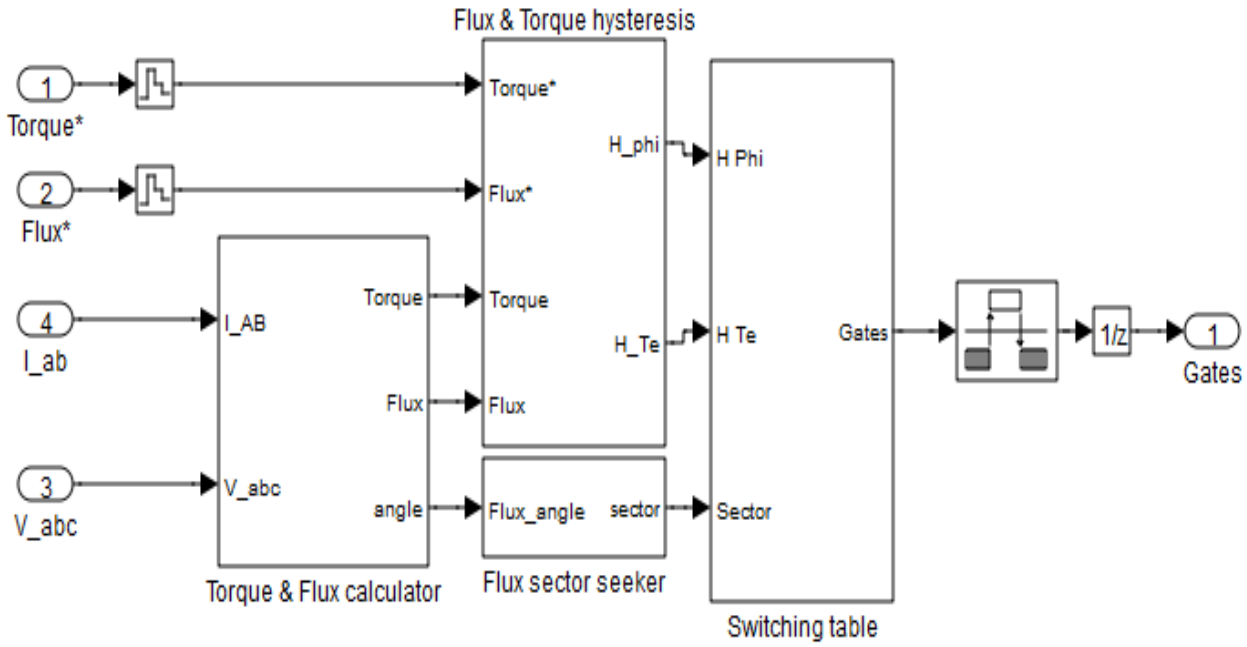


Fig.3.8(b) DTC Controller Block

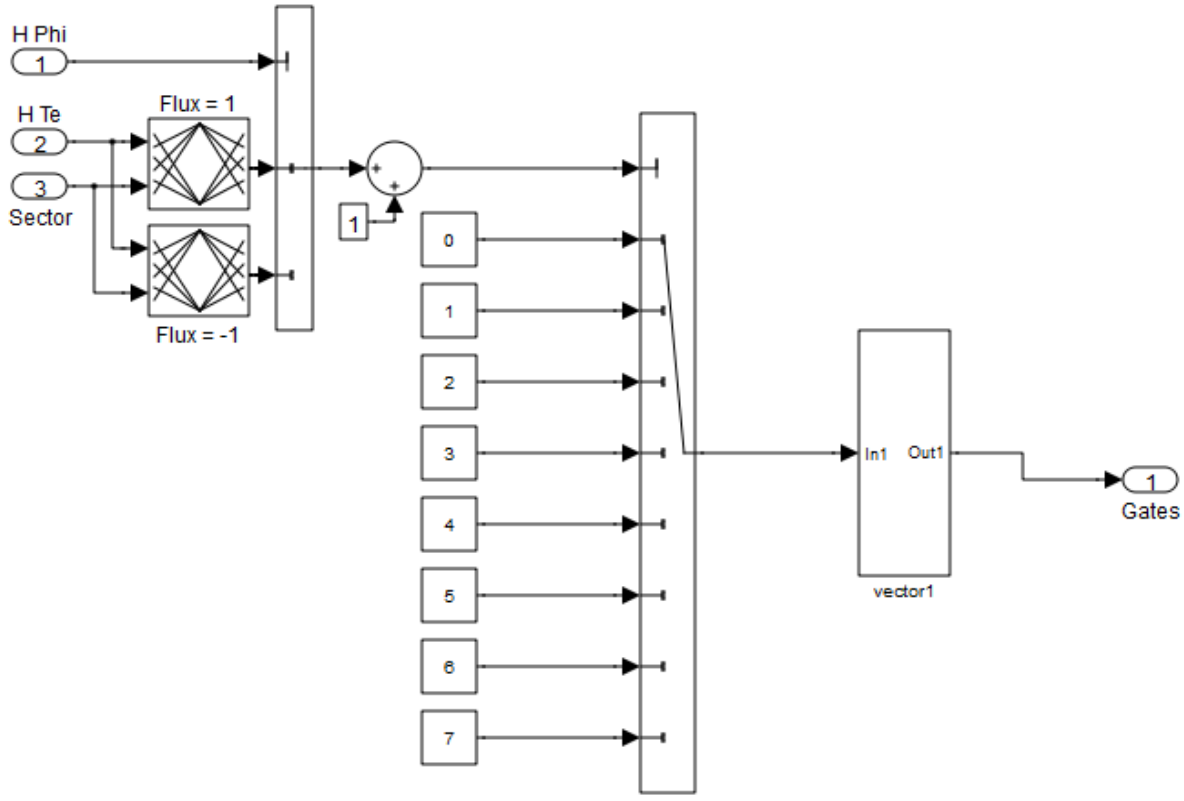


Fig.3.8(c) Selection of Switching Vector in Conventional DTC

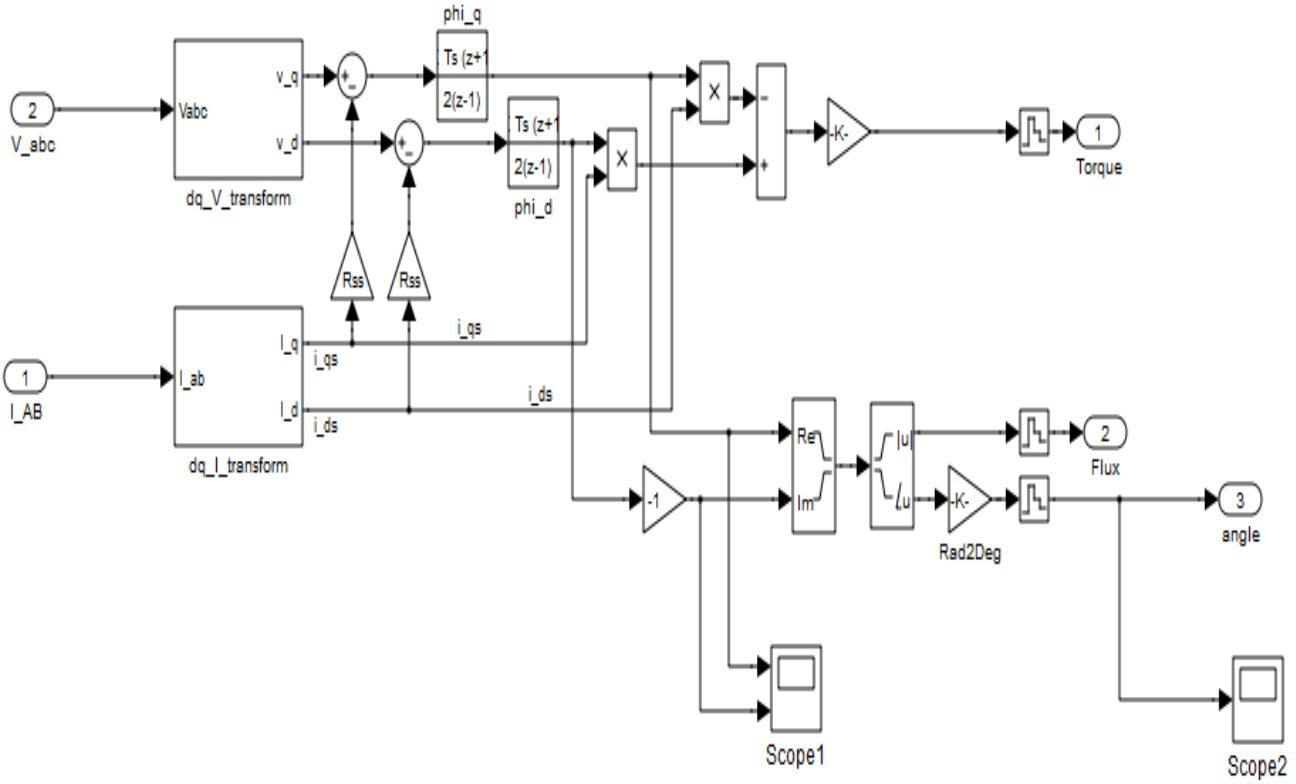


Fig.3.8(d) Torque and Flux Calculator

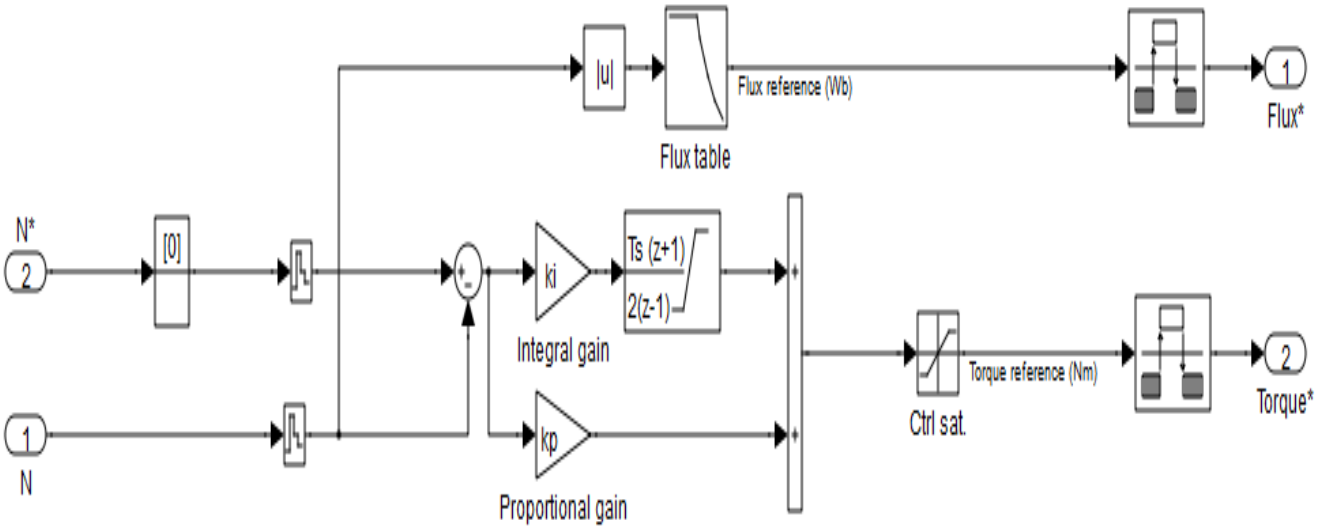


Fig.3.8(e) Speed Controller of Conventional DTC

In order to show the effectiveness of the control scheme, a simulation has been carried out for an induction motor. The control scheme is simulated with Matlab/Simulink, which is a tool for simulation. It has been considered:

i) The speed reference prescribed to (800; 1000) rpm at t = (0; 1.5) s,

ii) The load torque prescribed to (0; 12) Nm at t= (0;1.5) s with step variation.

The time variations of the main electrical and mechanical variables, specific to the presented drive (the stator current $i_{sa}$, the rotor speed N and the electromagnetic torque $T_e$) is obtained and it represent in Figure 3.9.

### 3.5.1 RESULTS AND DISCUSSION

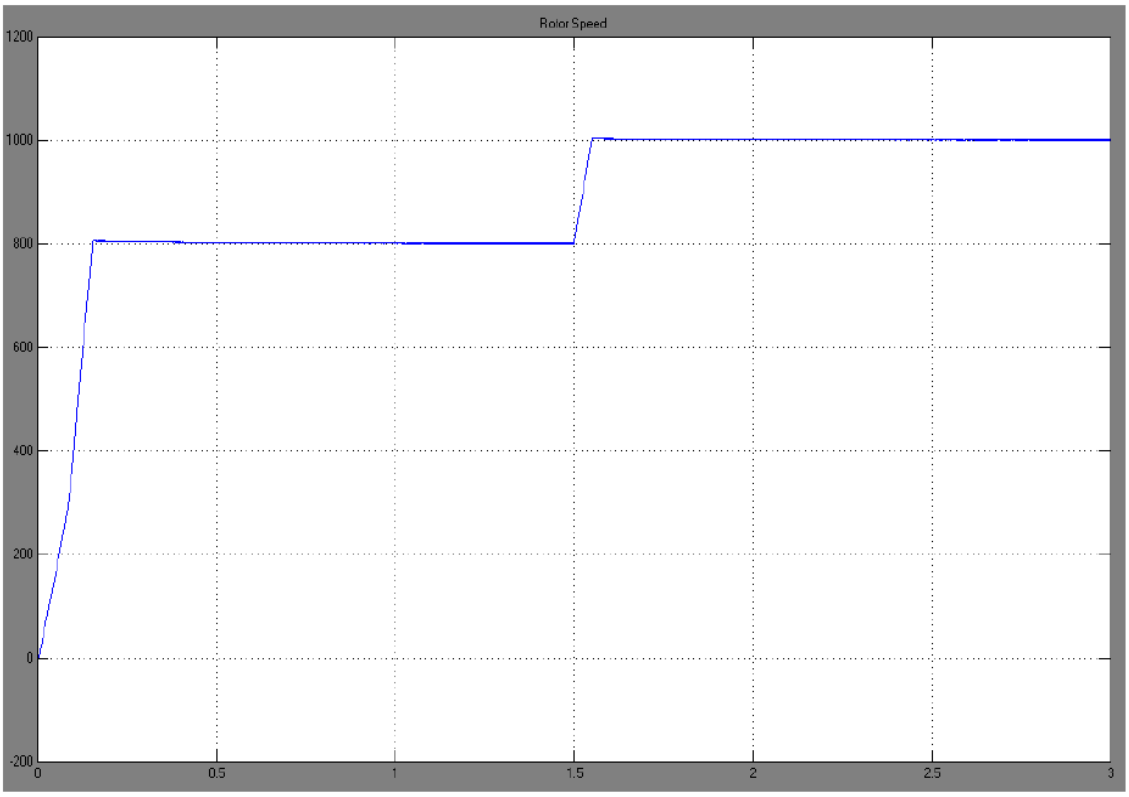


Fig.3.9(a) Rotor Speed (rpm) v/s Time (second)

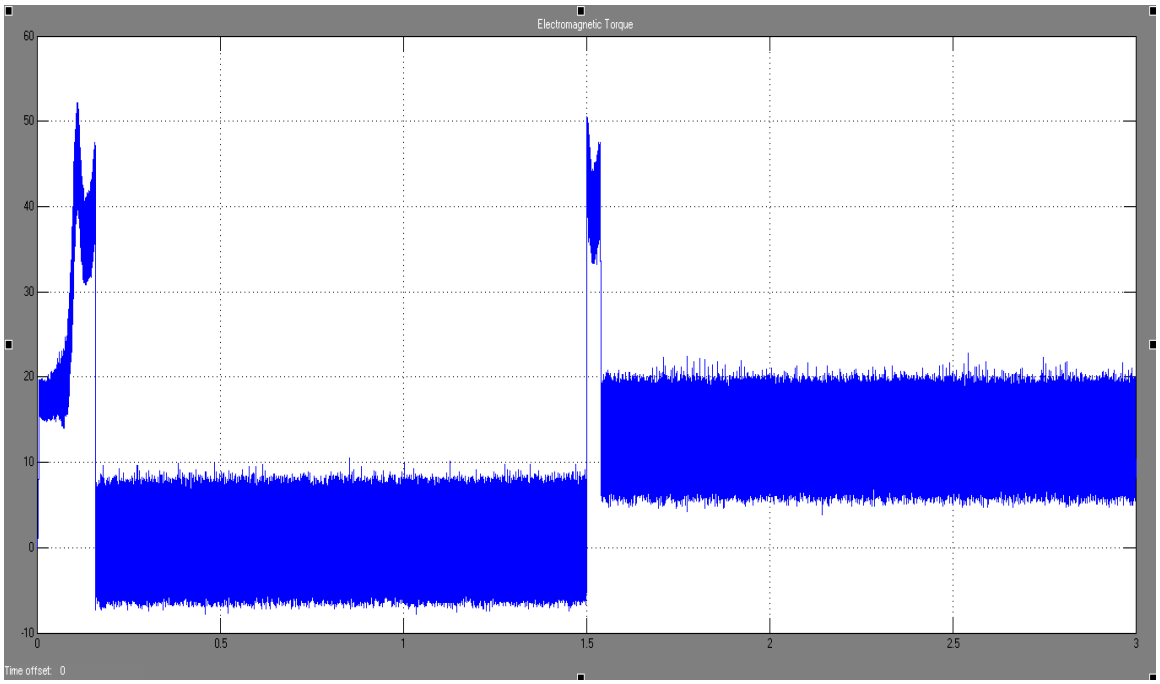


Fig.3.9(b) Electromagnetic Torque (Nm) v/s Time (second)

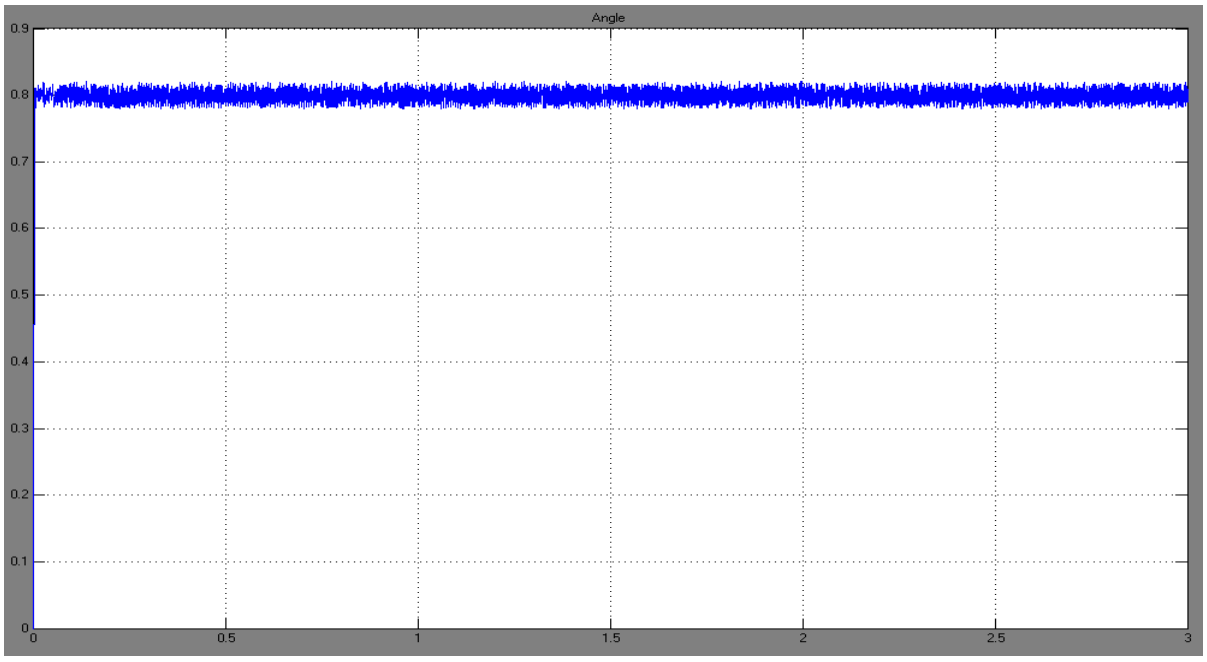


Fig.3.9(c) Stator Flux Linkage v/s Time (second)

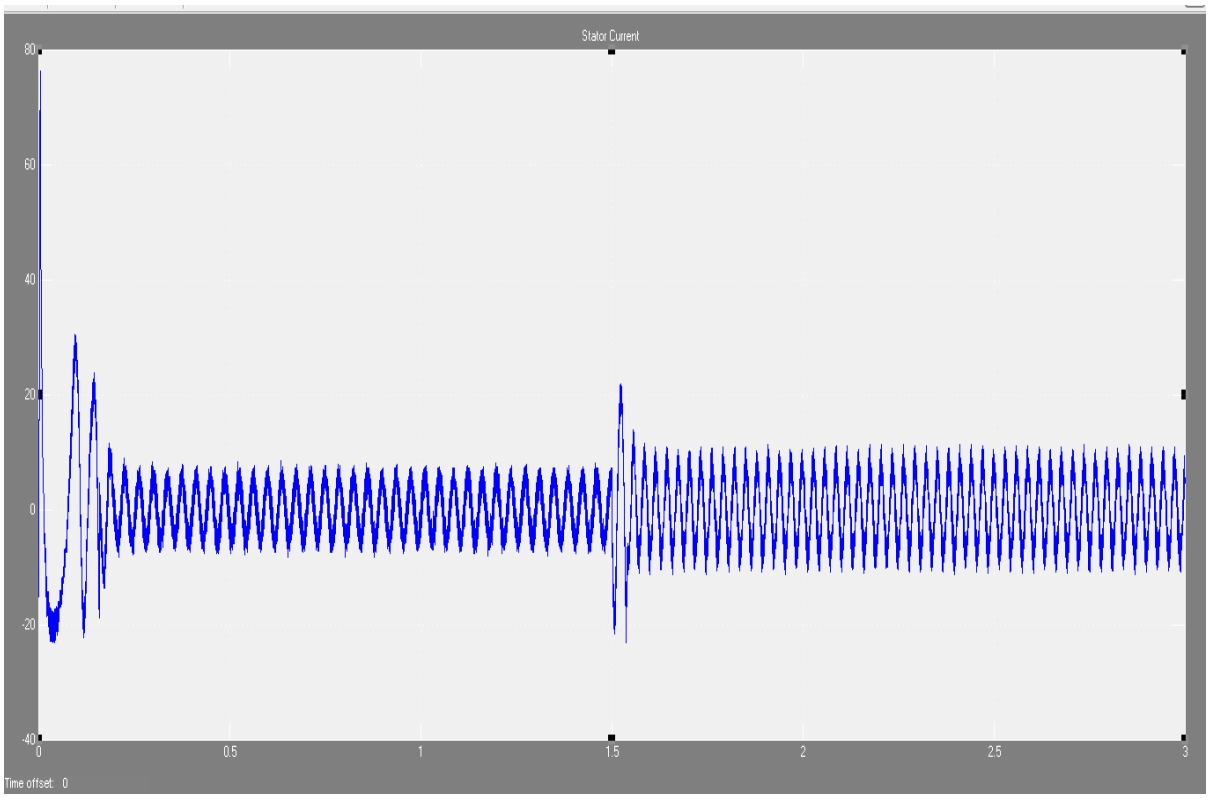


Fig.3.9(d) Stator Current (ampere) v/s Time (second)

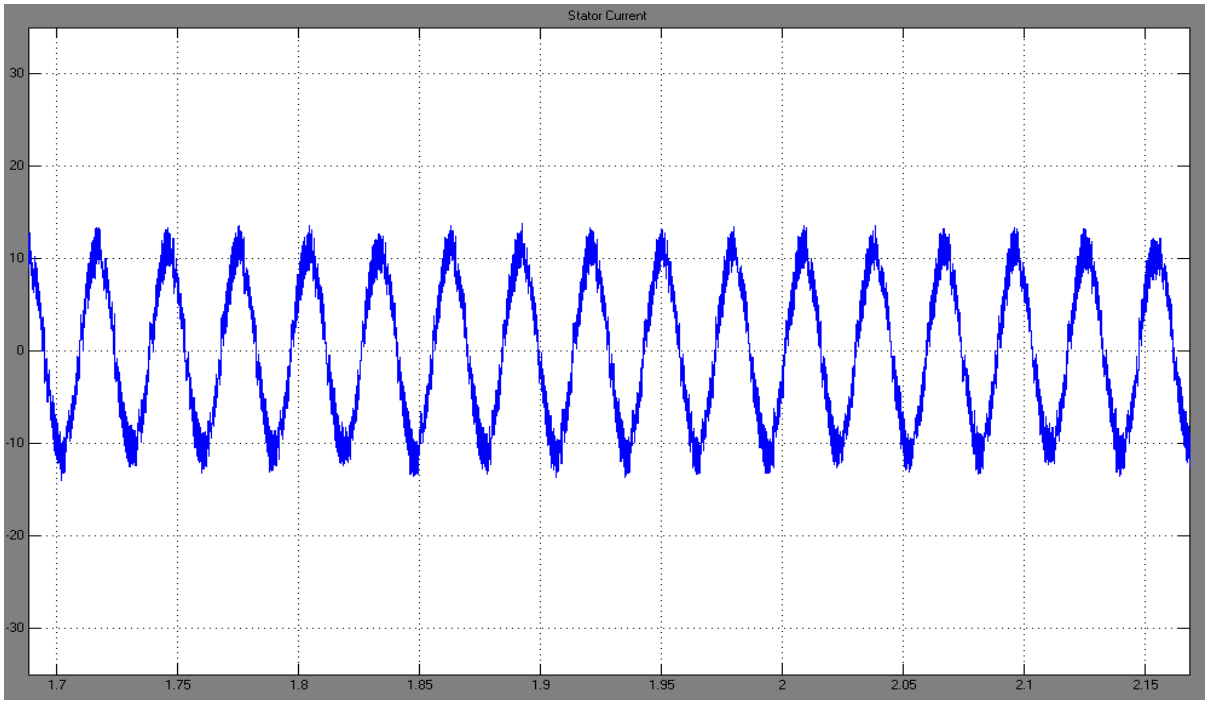


Fig.3.9(e) Stator Current (ampere) v/s Time (second)

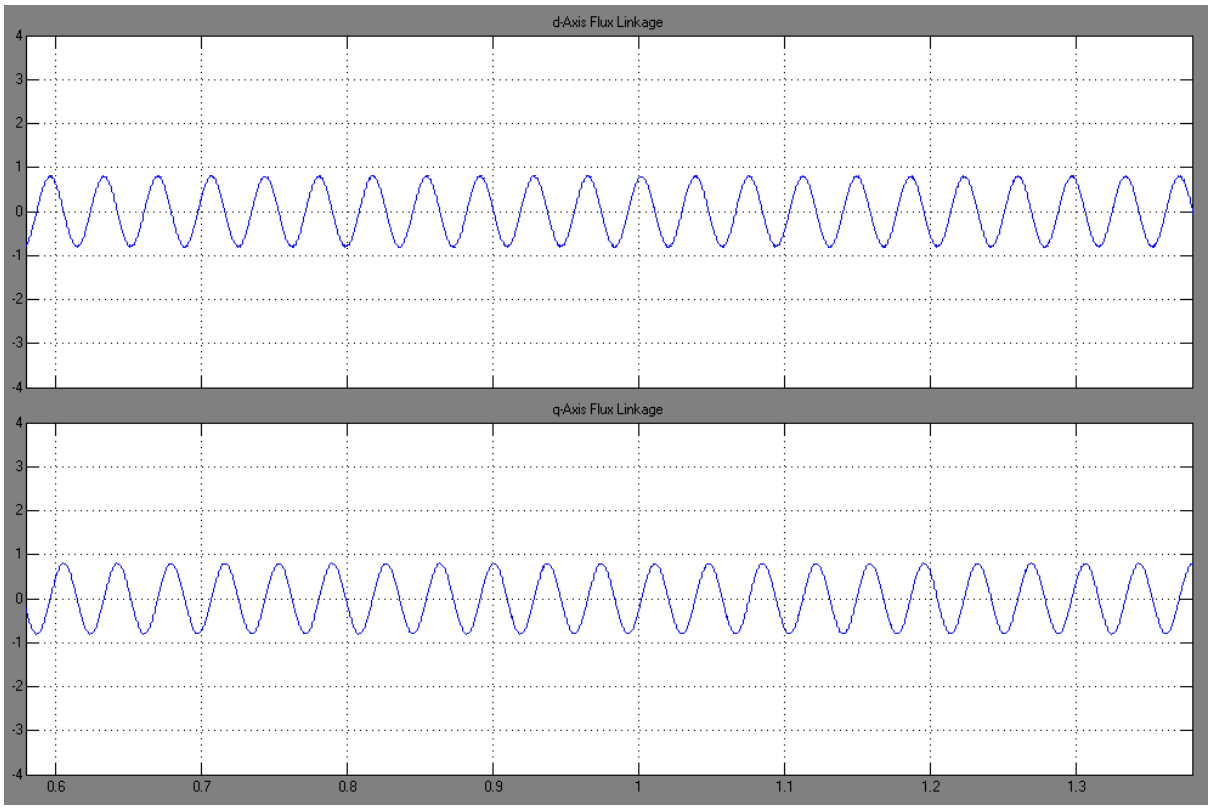


Fig.3.9(f) Direct and Quadrature Axis Flux Linkage v/s Time (second)

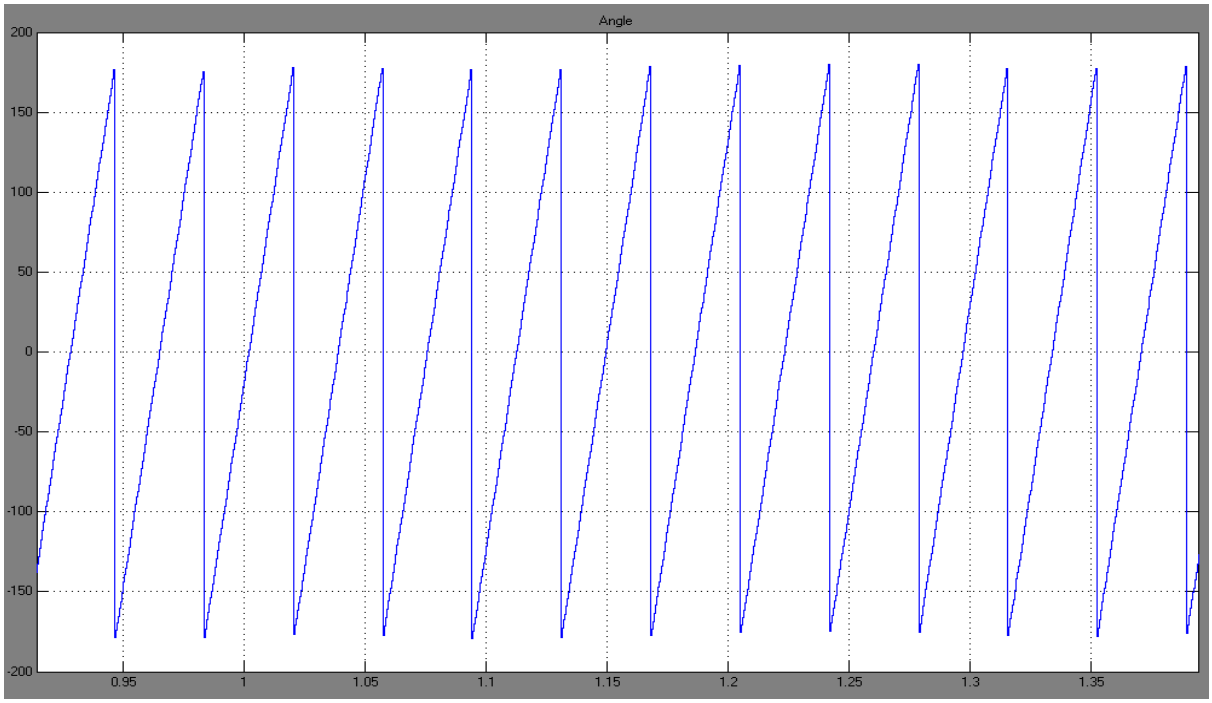


Fig.3.9(g) Angle of Flux linkage v/s Time (second)

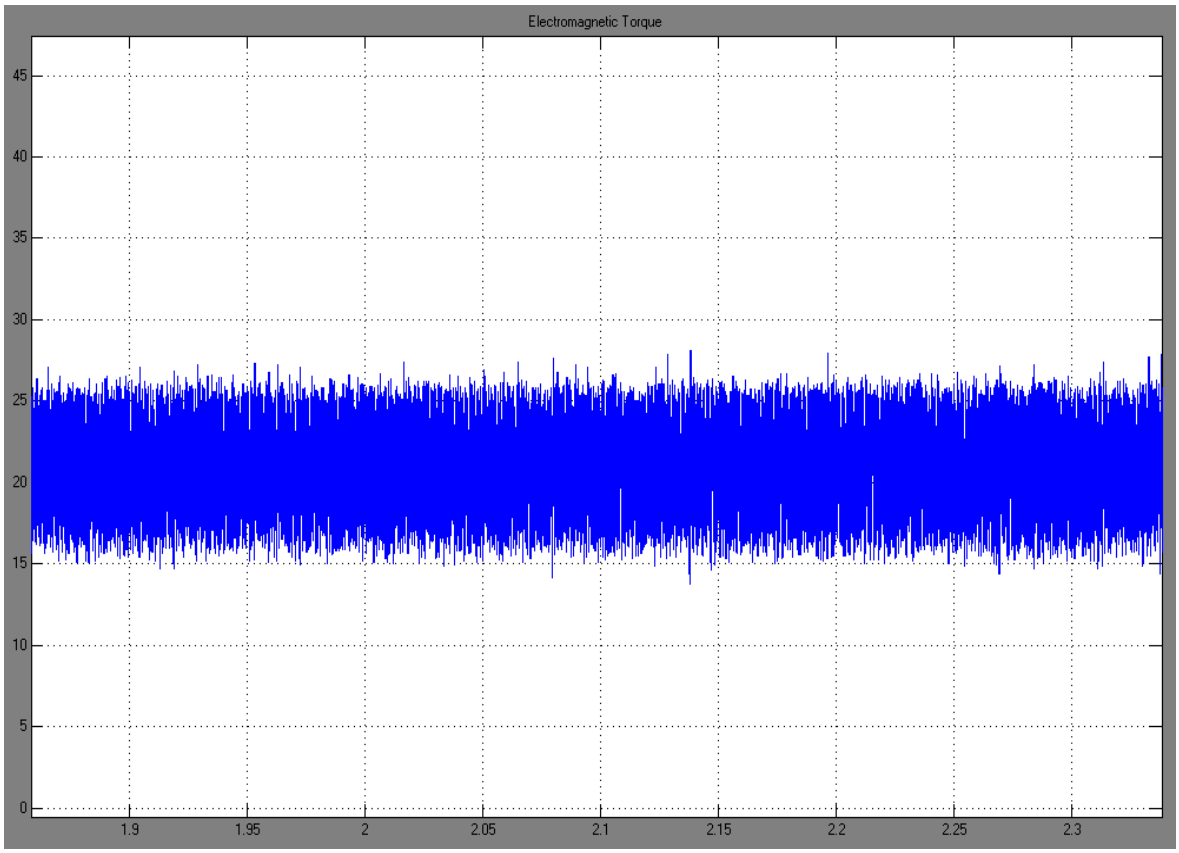


Fig.3.9(h) Torque Ripples in Conventional DTC

Figure 3.9(a) and 3.9(b) shows the speed torque responses of the induction motor at different conditions i.e. the speed command 800 rpm is given for 0 to 1.5 seconds and the load torque is changed at 1.5 second from 0 to 12 Nm. But the speed command is changed at 1.5 second from 800 rpm to 1000 rpm. Also, at 1.5 second from the Figure 3.9(b) it can see that if the speed command is changed suddenly then the induction motor produces a large electromagnetic torque, which is undesirable. From Figure 3.9(h), it can see that the torque ripple in case of conventional DTC is ($\pm$ 5) Nm.

## 3.6 CONCLUDING REMARKS

Conventional Direct torque control gives a fast torque response and better control over torque and flux. However the main drawback of this method comes from the fact that a voltage vector is applied continuously over a sample time. As a result, if the Torque error is small the torque developed after one cycle may not only reach the desired level but also overshoot. This leads to ripples in the torque developed and deteriorating performance. A simple way to reduce these ripples is to reduce the cycle time so that the motor state is sampled at a faster rate and torque overshooting its reference value is avoided. But this results in increased switching frequency and switching losses and expensive processing hardware.

# CHAPTER 4

# DIRECT TORQUE CONTROL OF INDUCTION MOTOR USING SPACE VECTOR MODULATION (SVM)

## 4.1 INTRODUCTION

Space vector modulation (SVM) is an algorithm for the control of pulse width modulation (PWM). It is an effective method of generating AC voltages to drive three phase AC motors at varying speed. There are various approaches of SVM that result in different output and computational requirements. One area of development is in the reduction of Total Harmonic Distortion (THD) due to the rapid switching. This algorithm of DTC is used for overcoming the drawbacks of classical DTC by voltage modulation application replacing look-up table of the voltage vector selection. The voltage modulation is based on SVM with constant switching frequency.

The SVM strategy is based on space vector representation of the converter AC side voltage. Contrary to conventional Pulse Width Modulation (PWM) method, in the SVM method there is no separate modulators for each phase**.** Alternatively, SVM method is incorporated with direct torque control DTC-SVM for induction motor drives to provide a constant inverter switching frequency.

The basis of the DTC-SVM strategy is the calculation of the required voltage space vector, to compensate the flux and torque errors. The main disadvantages of conventional DTC are high torque ripple and slow transient response to the step changes in torque during start-up. Several techniques have been developed to improve the torque performance. One of them is to reduce the ripples using SVM technique. The torque ripple for this DTC-SVM is significantly reduced and switching frequency is maintained constant. SVM is based on the switching between two adjacent boundaries of active vectors and a zero space vector. SVM is one of the preferred real-time modulation techniques and is widely used for digital control of voltage source inverters.

## 4.2 SWITCHING STATES OF TWO LEVEL INVERTER

A three phase inverter as shown in Figure 4.1 must be controlled so that both switches in the same leg should not be turned ON otherwise at the same time the DC supply would be shorted. This requirement may be met by the complementary operation of the switches within a leg i.e. if $T_1$ is on then $T_4$ is off and vice versa. Also, we see in the Table 4.1, switching state '1' denotes that the upper switch in an inverter leg is ON and the inverter terminal voltage ($V_{AN}$, $V_{BN}$ and $V_{CN}$) is positive ($+V_D$) while '0' indicates that the inverter terminal voltage is zero due to the conduction of the lower switch. This leads to eight possible switching vectors for the inverter, $V_0$ through $V_7$ with six active switching vectors and two zero vectors. The terminal voltage of 'A' with respect to negative of the DC supply is considered, and $V_{AN}$ is determined by a set of the switches in each leg, consisting of $T_1$ and $T_4$ as shown in Table 4.1. When the switching devices $T_1$ and $T_4$ and their anti-parallel diodes are off, which are not shown in diagram, $V_{AN}$ is indeterminate. Such a situation is not encountered in practice and, hence, has not been considered. The switching for the sets of 'B' and 'C' leg of the two level inverter as shown in Figure 4.1 can be similarly derived.

$$\begin{cases} V_{AB} = V_{AN} - V_{BN} \\ V_{BC} = V_{BN} - V_{CN} \\ V_{CA} = V_{CN} - V_{AN} \end{cases} \tag{4.1}$$

And machine phase voltages for a balanced system are:

$$\begin{cases} V_{AN} = \frac{(V_{AB} - V_{CA})}{3} \\ V_{BN} = \frac{(V_{BC} - V_{AB})}{3} \\ V_{CN} = \frac{(V_{CA} - V_{BC})}{3} \end{cases} \tag{4.2}$$

With the help of above set of equations, q-axis and d-axis voltages are given by:

$$V_{qs} = V_{AN} \tag{4.3}$$

$$V_{ds} = \frac{1}{\sqrt{3}} (V_{CN} - V_{BN}) = \frac{1}{\sqrt{3}} V_{CB} \tag{4.4}$$

The inverter create distinct discrete set of the stator-voltage consisting of the resultant of $V_{qs}$ and $V_{ds}$.

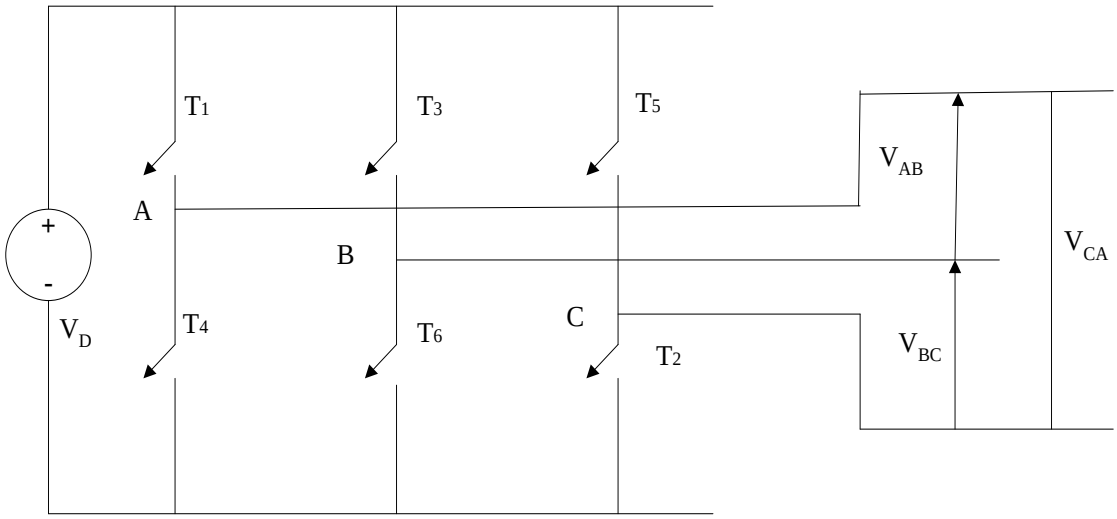


Fig.4.1 Two Level Inverter

Table 4.1 Definition of Switching States

| Switching State | Leg A | | | Leg B | | | Leg C | | |
|---|---|---|---|---|---|---|---|---|---|
| | $T_1$ | $T_4$ | $V_{AN}$ | $T_3$ | $T_6$ | $V_{BN}$ | $T_5$ | $T_2$ | $V_{CN}$ |
| 1 | On | Off | $V_D$ | On | Off | $V_D$ | On | Off | $V_D$ |
| 0 | Off | On | 0 | Off | On | 0 | Off | On | 0 |

Table 4.2 Space Vectors, Switching States and On State Switches

| Vector | $T_1$ | $T_3$ | $T_5$ | $T_4$ | $T_6$ | $T_2$ | $V_{AB}$ | $V_{BC}$ | $V_{CA}$ | |
|---|---|---|---|---|---|---|---|---|---|---|
| $V_0$={000} | OFF | OFF | OFF | ON | ON | ON | 0 | 0 | 0 | Zero Vector |
| $V_1$={100} | ON | OFF | OFF | OFF | ON | ON | $V_D$ | 0 | $V_D$ | Active Vector |
| $V_2$={110} | ON | ON | OFF | OFF | OFF | ON | 0 | $V_D$ | $V_D$ | Active Vector |
| $V_3$={010} | OFF | ON | OFF | ON | OFF | ON | $V_D$ | $V_D$ | 0 | Active Vector |
| $V_4$={011} | OFF | ON | ON | ON | OFF | OFF | $V_D$ | 0 | $V_D$ | Active Vector |
| $V_5$={001} | OFF | OFF | ON | ON | ON | OFF | 0 | $V_D$ | $V_D$ | Active Vector |
| $V_6$={101} | ON | OFF | ON | OFF | ON | OFF | $V_D$ | $V_D$ | 0 | Active Vector |
| $V_7$={111} | ON | ON | ON | OFF | OFF | OFF | 0 | 0 | 0 | Zero Vector |

## 4.3 SVM WITH TWO LEVEL INVERTER

To implement space vector modulation a reference signal $V^*$ is sampled with a sampling time $T_s$ ($T_s = 1/f_s$). The single reference signal may be generated from three separate phase references using the q-d transform i.e. with the help of Park's Transformation. The reference vector is then synthesized using a combination of the two adjacent active switching vectors and one or both of the zero vectors. Various strategies of selecting the order of the vectors and which zero vectors to use exist. Strategy selection will affect the harmonic content and the switching losses. This modulation strategy is particularly designed to work with voltage commands expressed in terms of q-d variables. A three phase two level converters provides eight possible switching states

made up six active and two zero switching states. SVM switching rules of $V_s$ should be a circle, only one switching per state transition. The final state of one sample must be the initial state of the next sample, this rules help in limiting the number of switching actions and there is a reduction in the switching losses.

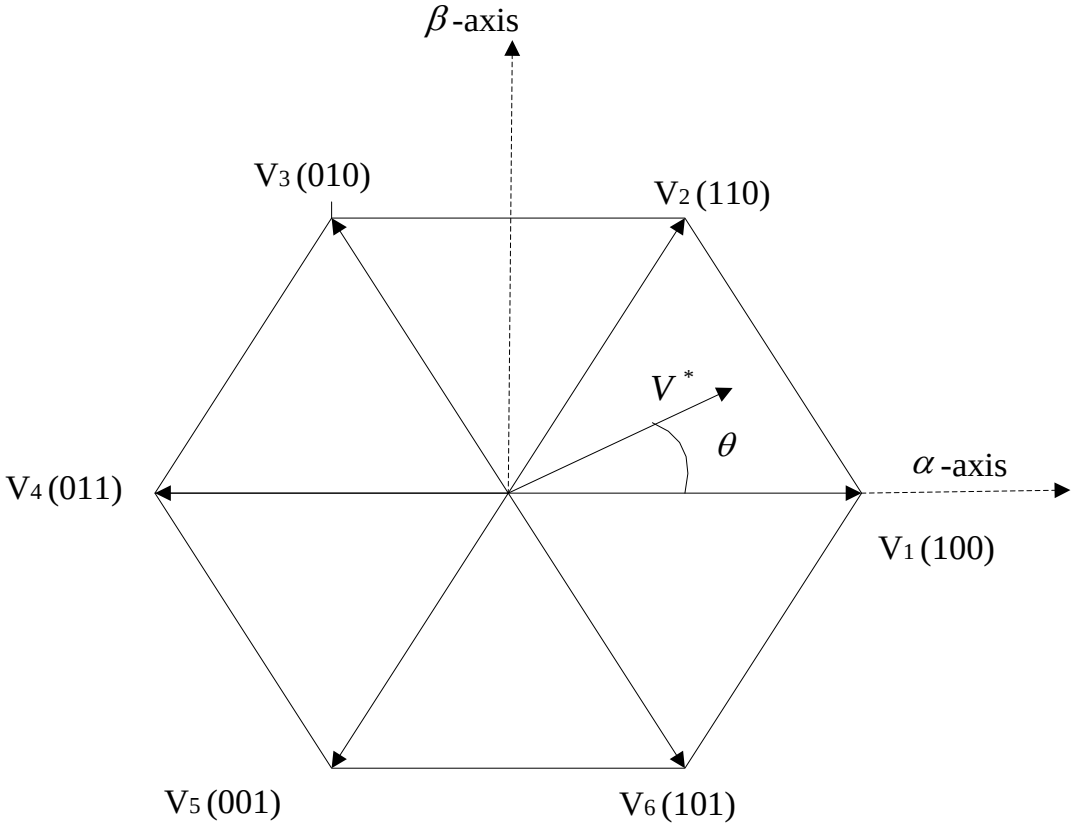


Fig.4.2 Space Vector Diagram For Two Level Inverter.

Space vector modulation strategy is particularly designed to work with voltage commands expressed in terms of q-d variables. In particular, in this strategy, voltage commands expressed in a stationary reference frame are sampled at the beginning of each switching cycle, and then the inverter semiconductors are switched in such a way that the fast average of the actual q-axis and d-axis voltages in the stationary reference frame are obtained over the ensuing switching period. Let the operation of the inverter is three-phase balanced, we have:

$$V_{AO}(t) + V_{BO}(t) + V_{CO}(t) = 0 \qquad (4.5)$$

Where, $V_{AO}$, $V_{BO}$, and $V_{CO}$ are the instantaneous phase voltages. From mathematical point of view, one of the phase voltages is redundant since for given any two phase voltages, the third one can be readily calculated for balanced system. Therefore, it is possible to transform the three-phase variables to equivalent two-phase variables:

$$\begin{bmatrix} V_\alpha \\ V_\beta \end{bmatrix} = \frac{2}{3}\begin{bmatrix} 1 & -\frac{1}{2} & -\frac{1}{2} \\ 0 & -\frac{\sqrt{3}}{2} & \frac{\sqrt{3}}{2} \end{bmatrix}\begin{bmatrix} V_{AO}(t) \\ V_{BO}(t) \\ V_{CO}(t) \end{bmatrix} \quad (4.6)$$

$$V(t) = V_\alpha(t) + j\, V_\beta(t) \quad (4.7)$$

$$|V^*| = \sqrt{V\alpha^2 + V_\beta{}^2} \quad \text{and } \Phi = \tan^{-1}\frac{V_\beta}{V_\alpha}$$

Put the value of Equation (4.6) into Equation (4.7), we have:

$$V(t) = \frac{2}{3}\left[V_{AO}(t)e^{j0} + V_{BO}(t)e^{\frac{2\pi}{3}} + V_{CO}(t)e^{\frac{4\pi}{3}}\right] \quad (4.8)$$

The space vector for all six active vectors can be derived by the following expression:

$$V_k = V_D\, e^{j(k-1)\pi/3},\ k = 1, 2,.....6 \quad (4.9)$$

The zero vector $V_0$ has two switching states [111] and [000], seems to be redundant. The relationship between the space vectors and their corresponding switching states is given in Table 4.2. The zero and active vectors do not move in space, and thus they are referred to as stationary vectors. On the contrary, the reference vector $V^*$ in Figure 4.2 rotates in space at an angular velocity

$$\omega = 2\pi f_1 \quad (4.10)$$

Where, $f_1$ is the fundamental frequency of the inverter output voltage. The angular displacement between $V^*$ and the α-axis of the α-$\beta$ plane can be obtained as:

$$\theta(t) = \int_0^t \omega(t)dt + \theta(0) \quad (4.11)$$

For a given magnitude and position, $V^*$ can be synthesized by three nearby stationary vectors, based on which the switching states of the inverter can be selected and gate signals for the active switches can be generated. When $V^*$ passes through sectors one by one, different sets of switches will be turned ON or OFF. As a result, when $V^*$ rotates one

revolution in space, the inverter output voltage varies one cycle. The inverter output frequency corresponds to the rotating speed of $V^*$, while its output voltage can be adjusted by the magnitude of $V^*$.

## 4.4 SPACE VECTOR DWELL TIME CALCULATIONS

The basis of the DTC-SVM strategy is the calculation of the required voltage space vector, required to compensate the flux and torque errors at each sample period. As mentioned earlier, the reference space vector ($V^*$) can be synthesized by three stationary vectors. The dwell time for the stationary vectors essentially represents the duty-cycle time (ON-state or OFF-state time) of the chosen switches during a sampling period ($T_s$) of the modulation scheme. The term duty cycle describes the proportion of ON time to the regular interval or 'period' of time; a low duty cycle corresponds to low power. Duty cycle is expressed in percent. The dwell time calculation is based on "volt-second" balancing principle, that is, the product of the reference voltage $V^*$ and sampling period $T_s$ equals the sum of the voltage multiplied by the time interval of chosen space vectors.

Assuming that the sampling period $T_s$ is sufficiently small, the reference vector ($V^*$) can be considered constant during $T_s$. Under this assumption, $V^*$ can be approximated by two adjacent active vectors and one zero vector. For example, when $V^*$ falls into sector 1 as shown in Figure 4.3, it can be synthesized by $V_1$, $V_2$, and $V_0$.

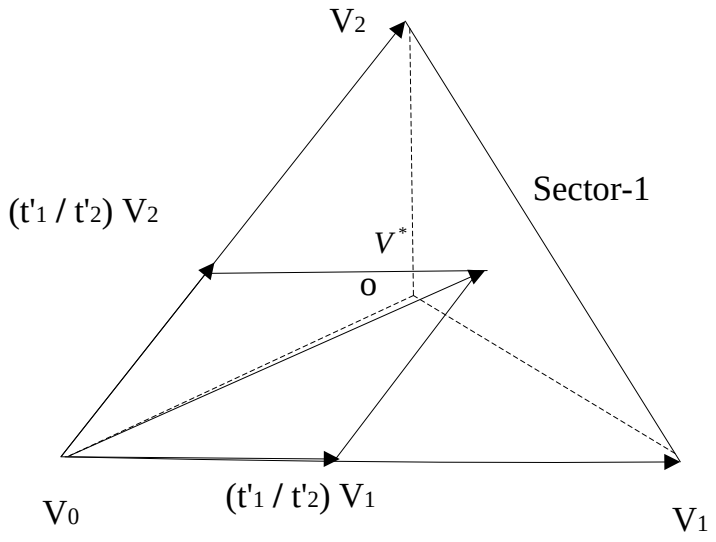


Fig.4.3 Reference Vector **(**$V^*$) Synthesized By $V_1$, $V_2$ and $V_0$.

Table 4.3 Values of Space Vector

| Space Vector | Vector Definition |
|---|---|
| $V_0$ | $V_0 = 0$ |
| $V_1$ | $V_1 = \frac{2}{3} V_D e^{j0}$ |
| $V_2$ | $V_2 = \frac{2}{3} V_D e^{j\frac{\pi}{3}}$ |
| $V_3$ | $V_3 = \frac{2}{3} V_D e^{j\frac{2\pi}{3}}$ |
| $V_4$ | $V_4 = \frac{2}{3} V_D e^{j\frac{3\pi}{3}}$ |
| $V_5$ | $V_5 = \frac{2}{3} V_D e^{j\frac{4\pi}{3}}$ |
| $V_6$ | $V_6 = \frac{2}{3} V_D e^{j\frac{5\pi}{3}}$ |
| $V_7$ | $V_7 = 0$ |

In the above Table 4.3 we get the values of space vector according to the Table 4.2

The volt-second balancing equation is given by:

$$V^*T_s = V_1t_1' + V_2t_2' + V_0t_0' \quad (4.12)$$

$$T_s = t_1' + t_2' + t_0'$$

Where, $t_1'$, $t_2'$ and $t_0'$ are the dwell times for the vectors $V_1$, $V_2$ and $V_0$, respectively.

The space vectors in Equation 4.12 can be expressed as if sector 1 is selected

$$V_1 = 2/3V_D,\ V_2 = 2/3V_De^{j\pi/3},\ \text{and}\ V_0 = 0 \quad (4.13)$$

Generally, we write $V^*$ can be written as:

$$V^* = V^*\ e^{j\theta} \quad (4.14)$$

The values of voltage space vector for different sectors are given in Table 4.3. Substituting Equations 4.13 and Equation 4.14 into Equation 4.12 and then splitting the resultant equation into the real (α-axis) and imaginary (β-axis) components in the α–β plane, we have

*Real Axis-*

$$V^* (\cos \theta)\, T_s = 2/3 V_D t_1' + 1/3 V_D t_2' \quad (4.15)$$

*Imaginary Axis-*

$$V^* (\sin \theta)\, T_s = \frac{1}{\sqrt{3}} V_D\, t_2' \quad (4.16)$$

By solving Equation 4.15 and Equation 4.16 with $T_s = t_1' + t_2' + t_0'$ gives

$$t_1' = \frac{\sqrt{3}}{V_D} T_s\, V^* \sin\left(\frac{\pi}{3} - \theta\right) \quad (4.17)$$

$$t_2' = \frac{\sqrt{3}}{V_D} T_s\, V^* \sin(\theta) \qquad \text{for} \qquad 0 \leq \theta < \frac{\pi}{3} \quad (4.18)$$

$$t_0' = T_s - t_1' - t_2' \quad (4.19)$$

Although Equation 4.17, Equation 4.18 and Equation 4.19 are derived when $V^*$ is in sector 1, it can also be used when $V^*$ is in other sectors provided that a multiple of $\pi/3$ is subtracted from the actual angular displacement $\theta$ such that the modified angle $\theta$ falls into the range between zero and $\pi/3$ for use in the equation, that is,

$$\theta' = \theta - (k - 1)\frac{\pi}{3} \qquad \text{for} \qquad 0 \leq \theta < \frac{\pi}{3} \quad (4.20)$$

Where k = 1, 2. . . 6 for sectors 1, 2 . . . 3, respectively.

Table 4.4 Position of $V^*$ Location and Dwell Times

| $V^*$ location | $\theta = 0$ | $0 < \theta < \frac{\pi}{6}$ | $\theta = \frac{\pi}{6}$ | $\frac{\pi}{6} < \theta < \frac{\pi}{3}$ | $\theta = \frac{\pi}{3}$ |
|---|---|---|---|---|---|
| Dwell Times | $t_1' > 0$<br>$t_2' = 0$ | $t_1' > t_2'$ | $t_1' = t_2'$ | $t_1' < t_2'$ | $t_1' = 0$<br>$t_2' > 0$ |

## 4.5 MODULATION INDEX

When describing the space-vector modulator algorithm, the q-axis and d-axis modulation indexes are defined as the q-axis and d-axis voltages in the stationary reference frame normalized to the DC voltage respectively as:

$$m_q^s = V_q^s / V_D \quad (4.21)$$

$$m_d^s = V_d^s / V_D \quad (4.22)$$

It is convenient to define the commanded modulation indexes as:

$$m_q^{s*} = V_q^{s*} / V_D \quad (4.23)$$

$$m_d^{s*} = V_d^{s*} / V_D \quad (4.24)$$

Assuming that the DC voltage is constant or at least slowly varying compared to the switching frequency. It is apparent that the fast average of the q-axis and d-axis voltage will be equal to the commanded voltages if the fast average of the q-axis and d-axis modulation index is equal to the commanded modulation index. The space-vector modulation strategy can now be explained in terms of the space vector diagram illustrated in Figure 4.4. Therein, the q-axis and d-axis modulation index vector corresponding to each of the eight possible switching states of the converter is shown in Table 4.5. The values of the q-axis and d-axis modulation index corresponding to the $i_{th}$ state, $m_{q,x}$ and $m_{d,x,}$ respectively, along with ON/OFF status of the inverter transistors corresponding to the state, are listed in Table 4.5. In order to determine the sequence of states required in order to achieve the desired modulation index for a switching cycle, the following steps are performed.

- Given the q-axis and d-axis voltage command in the stationary reference frame, the q-axis and d-axis modulation index command is calculated using [Equation (4.23) - Equation (4.24)].
- To limit the magnitude of the modulation index command to reflect the voltage limitation applied to the converter. The magnitude of the modulation index command is defined as:

$$m^* = \sqrt{\left(m_q^{s*}\right)^2 + \left(m_d^{s*}\right)^2} \tag{4.25}$$

In the stationary reference frame, the modulation index command vector has a magnitude of $m^*$ and rotates in the q-d plane at the desired frequency. The maximum $m^*$ that achieved without introducing low frequency harmonics corresponds to the radius of the largest circle that can be circumscribed within the boundaries of the hexagon connecting the switching state vectors in Figure 4.4. This radius is given by:

$$m_{max} = \frac{1}{\sqrt{3}} \tag{4.26}$$

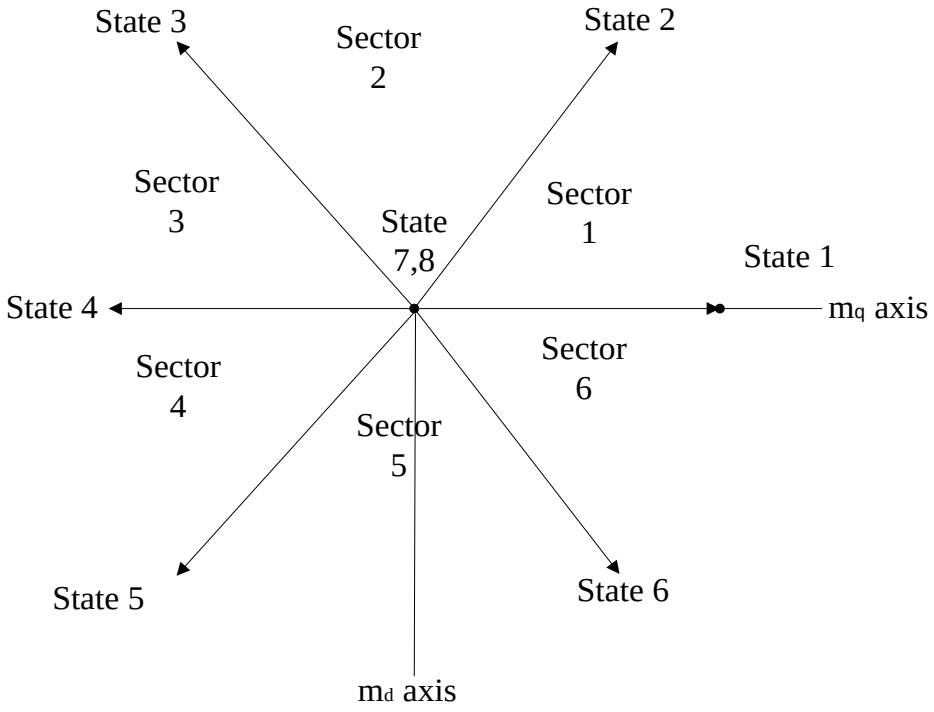


Fig.4.4 Space Vector Diagram with Axis of Modulation Index

Table 4.5 Modulation Indexes v/s State

| Switching States | A | B | C | $m_{q,x}$ | $m_{d,x}$ |
|---|---|---|---|---|---|
| 1 | 1 | 0 | 0 | 2/3 cos ($0^0$) | -2/3 sin ($0^0$) |
| 2 | 1 | 1 | 0 | 2/3 cos ($60^0$) | -2/3 sin ($60^0$) |
| 3 | 0 | 1 | 0 | 2/3 cos ($120^0$) | -2/3 sin ($120^0$) |
| 4 | 0 | 1 | 1 | 2/3 cos ($180^0$) | -2/3 sin ($180^0$) |
| 5 | 0 | 0 | 1 | 2/3 cos ($240^0$) | -2/3 sin ($240^0$) |
| 6 | 1 | 0 | 1 | 2/3 cos ($300^0$) | -2/3 sin ($300^0$) |
| 7 | 1 | 1 | 1 | 0 | 0 |
| 8 | 0 | 0 | 0 | 0 | 0 |

In Table 4.5 ‘A’, ‘B’ and ‘C’ are the legs of two the level inverter as shown in Figure 4.1. The limited modulation index command is next found as follows. First, the magnitude of the raw command is computed using Equation 4.25. Then, the modulation indexes are calculated as follows:

$$m_q^{**} = \begin{cases} m_q^* & m^* \le m_{max} \\ m_{max}\frac{m_q^*}{|m^*|} & m^* > m_{max} \end{cases} \quad (4.27)$$

$$m_d^{**} = \begin{cases} m_d^* & m^* \le m_{max} \\ m_{max}\frac{m_d^*}{|m^*|} & m^* > m_{max} \end{cases} \quad (4.28)$$

The next step is to compute the sector of the modulation index. This is readily calculated from:

$$\text{Sector} = \text{ceil}\left(\frac{\text{angle}\left(m_q^{**} - jm_d^{**}\right)^3}{\pi}\right) \quad (4.29)$$

Where, angle ( ) returns the angle of its complex argument and has a range of 0 to 2π, and ceil ( ) returns next greatest integer.

Equation 4.17, Equation 4.18 and Equation 4.19 can be also being written in terms of modulation index. Here, for convenience, modulation index can be denoted as 'm'

$$t_1' = m\ T \sin\left(\frac{\pi}{3} - \theta\right) \tag{4.30}$$

$$t_2' = m\ T \sin\theta \tag{4.31}$$

$$t_0' = T - t_1' - t_2' \tag{4.32}$$

Where, $$m = \sqrt{3}\left(\frac{V_m^*}{V_D}\right) \tag{4.33}$$

The maximum magnitude of the reference vector; $V_m^*$ corresponds to the radius of the largest circle that can be inscribed within the hexagon shown in Figure 4.2. Since the hexagon is formed by six active vectors having a length of $2V_D/3$, $V_m^*$ be obtained as:

$$V_m^* = \frac{2}{3} V_D \times \frac{\sqrt{3}}{2} = \frac{V_D}{\sqrt{3}} \tag{4.34}$$

Substituting Equation 4.34 into Equation 4.33 gives the maximum modulation index:

$$m_{max} = \frac{1}{\sqrt{3}}$$

From which the modulation index for the SVM scheme is in the range of

$$0 \leq m_{max} \leq \frac{1}{\sqrt{3}} \tag{4.35}$$

The maximum fundamental line-to-line voltage (rms) produced by the SVM scheme can be calculated by:

$$V_{m,SVM} = \sqrt{3}\left(\frac{V_m^*}{\sqrt{2}}\right) \tag{4.36}$$

Substitute the value of $V_m^*$ from Equation (4.34) in Equation (4.36), we get:

$$V_{m,SVM} = \sqrt{3} \times \frac{V_D}{\sqrt{3}} \times \left(\frac{1}{\sqrt{2}}\right) = 0.707\ V_D \tag{4.37}$$

Where, $\left(\frac{V_m^*}{\sqrt{2}}\right)$ is the maximum rms value of the fundamental phase voltage of the inverter.

## 4.6 OPERATING PRINCIPLE OF DTC-SVM

The operating principle of a variable speed electric drive controlled through the space vector modulation is presented in Figure 4.5

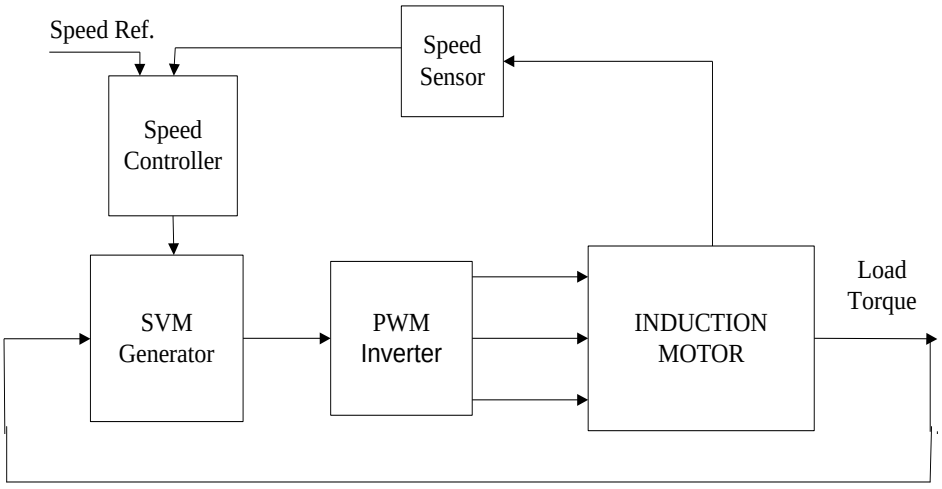


Fig.4.5 Operating Principle of Induction Motor Drive Controlled Through SVM Strategy

The actual speed is first compared with the reference speed for the closed loop speed control. The two PI controllers are used in speed controller which gives reference voltage and frequency to generate the three phase sinusoidal signal. These sinusoidal signals are used in SVM generator and based on the space vector position in the space, SVM calculate proper switching time for two consecutive switching vectors and also for zero switching vector and based on that switching vector, inverter gives supply to the induction motor.

## 4.7 SIMULATION MODEL OF DTC-SVM

To analyze the principle Figure 4.6(a), Figure 4.6(b) and Figure 4.6(c) show the model using both Simulink blocks and Sim Power Systems blocks. The supply of the induction motor is made from a three phase alternative voltage source with the help of the component using three phase rectifier, intermediate DC circuit, controlled three phase inverter and the elements which are introduced in Simulink scheme through Sim Power Systems pre-definite blocks.

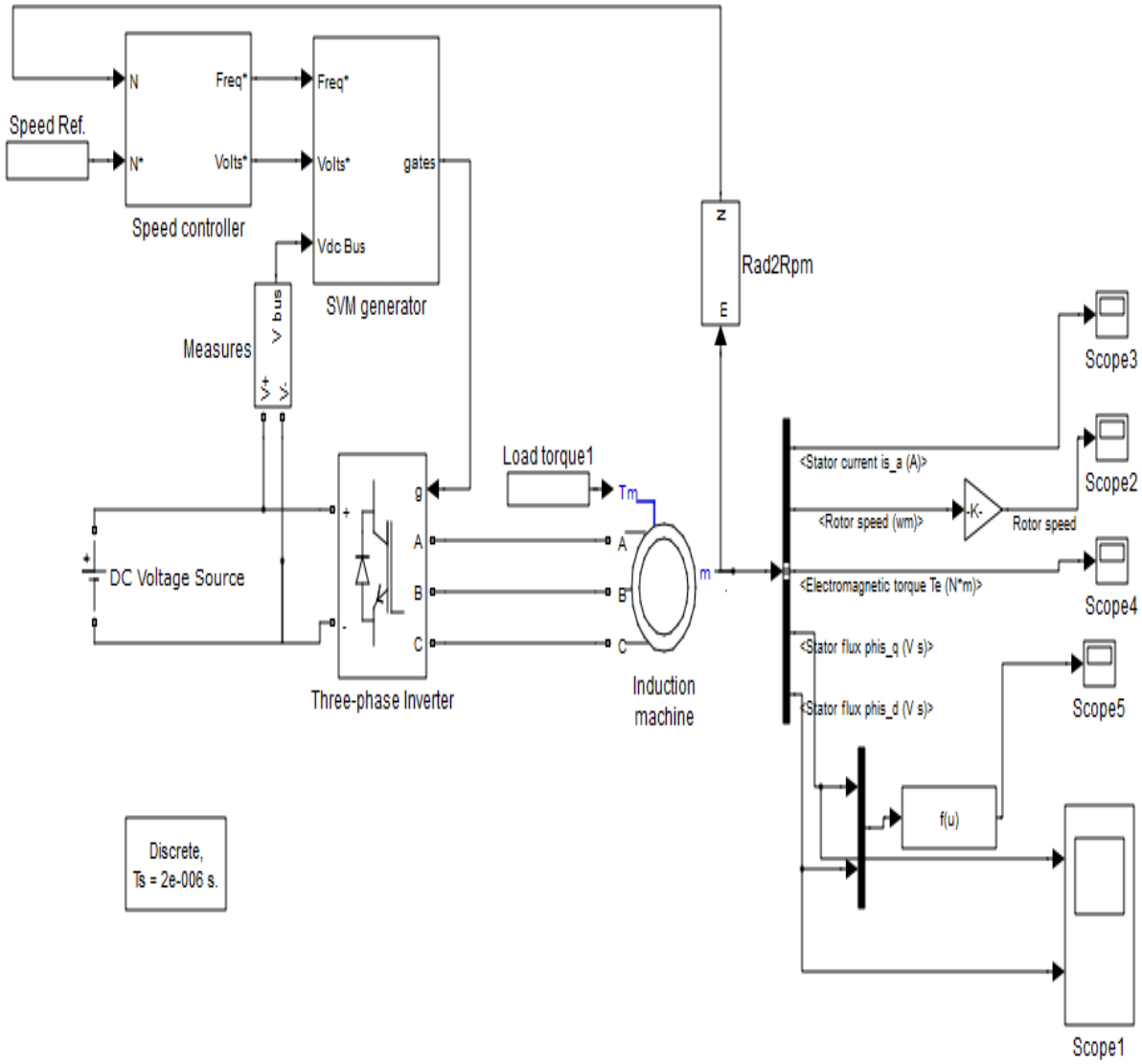


Fig.4.6(a) Simulation Model of DTC-SVM

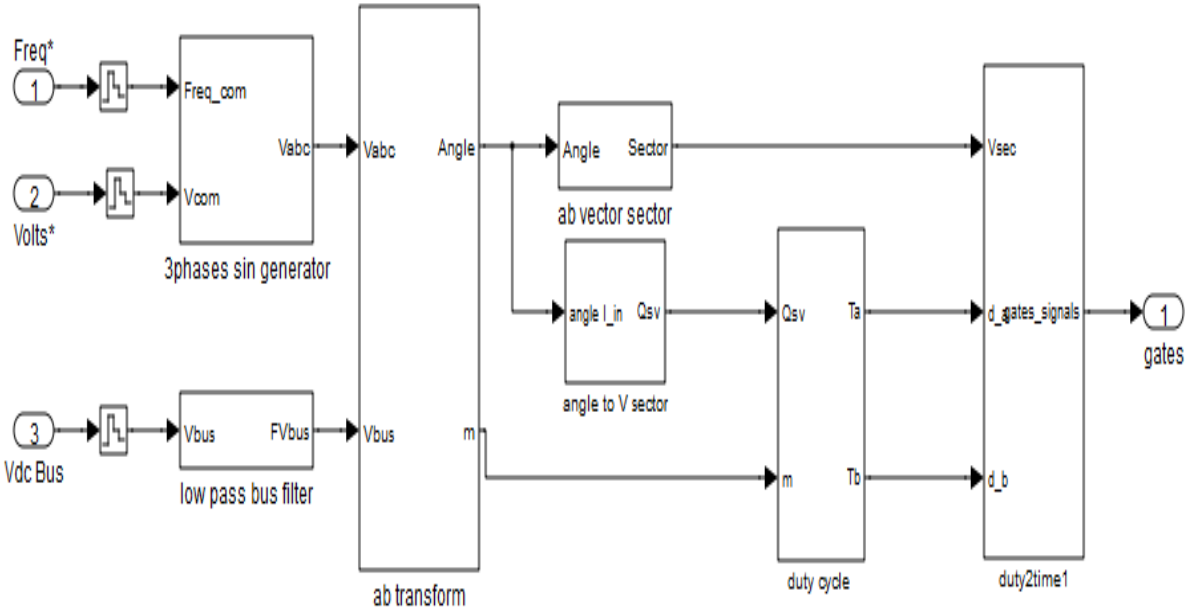


Fig.4.6(b) SVM Generator Block

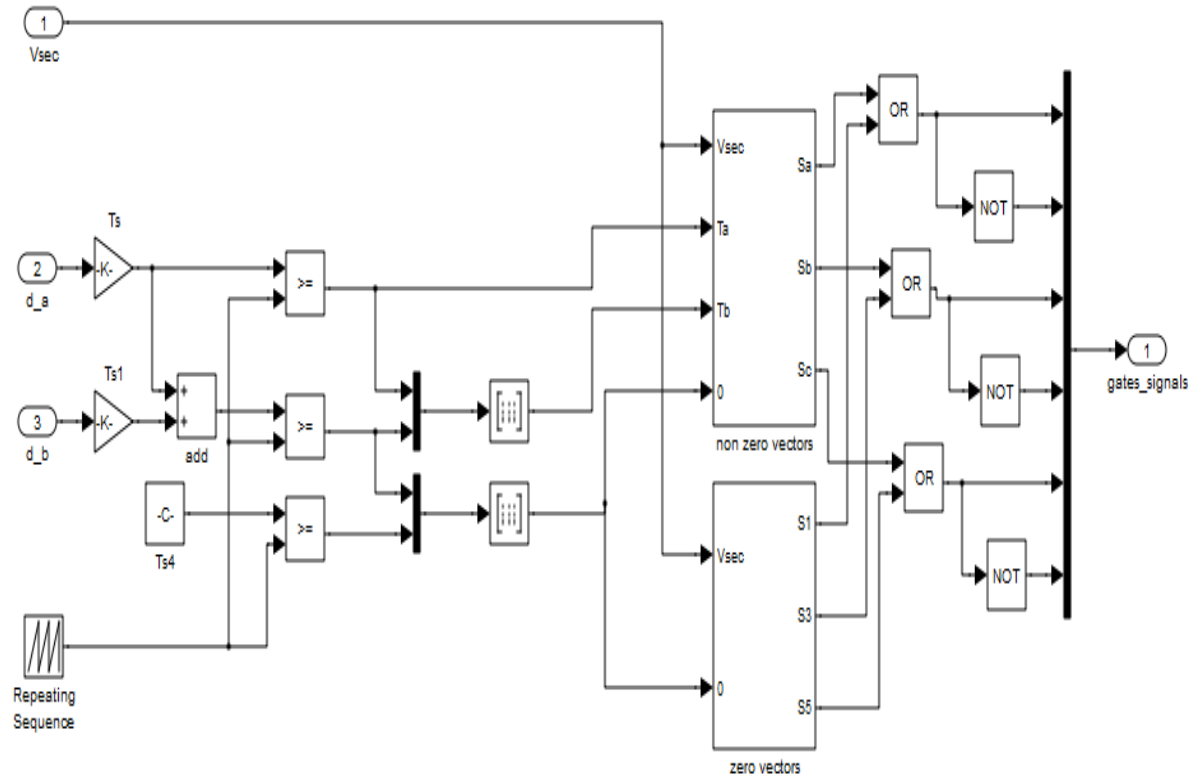


Fig. 4.6(c) Calculation of Dwell Time $t_0'$, $t_1'$, $t_2'$

### 4.7.1 SPEED CONTROLLER BLOCK

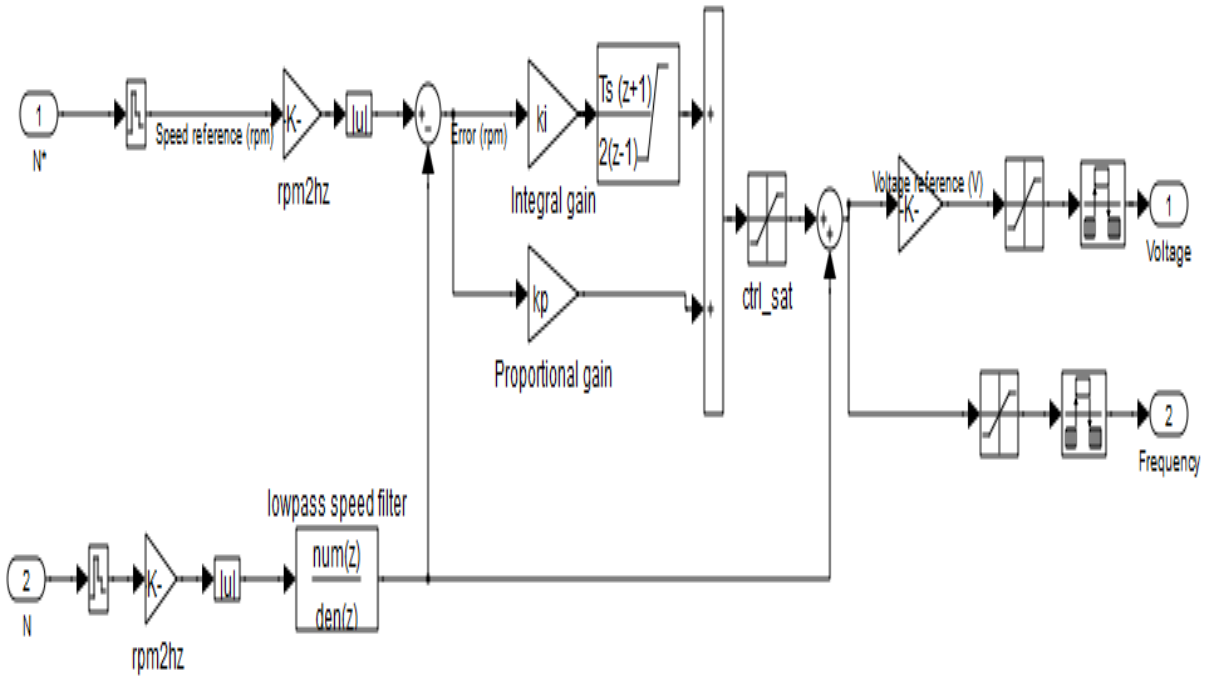


Fig.4.7 Speed Controller Block

The speed controller (Figure 4.7) has inputs as:

a) The reference speed *N** which is given by the Speed reference block,

b) The speed *N* obtained from the induction motor,

And output of the signals as:

a) *Freq.** (the reference frequency),

b) *Volts** (the reference voltage),

The first three output signals are the inputs to the SVM generator subsystem. The speed controller is based on a proportional integrator (PI) regulator which controls the motor slip. The slip value calculated by the PI regulator is added to the motor speed in order to produce the demanded inverter frequency. This frequency is also used to generate the required inverter voltage in order to maintain the motor V/f ratio constant.

### 4.7.2 DESCRIPTION OF SVM GENERATOR BLOCKS

The SVM generator, whose operating principle is presented in Figure 4.8, contains six blocks with the following functions:

- The three-phase generator is used to produce three sine waves with variable frequency and amplitude; the three signals maintain the difference of $120^0$.
- The $\alpha - \beta$ transformation converts variables from the three-phase system to the two-phase $\alpha - \beta$ system.
- The $\alpha - \beta$ vector sector is used to find the sector in the $\alpha - \beta$ plane for the voltage vector; this plane is divided into six different sectors spaced by $60^0$.
- The ramp generator is used to produce a unitary ramp at the PWM switching frequency; this ramp is used as a time base for the switching sequence
- The switching time calculator is used to calculate the timing of the voltage vector applied to the motor
- The gates logic compares the ramp and the gate timing signals to activate the inverter switches at the proper time

The schematic for the simulation of the component blocks in Matlab/Simulink is done in Figure 4.6(a).

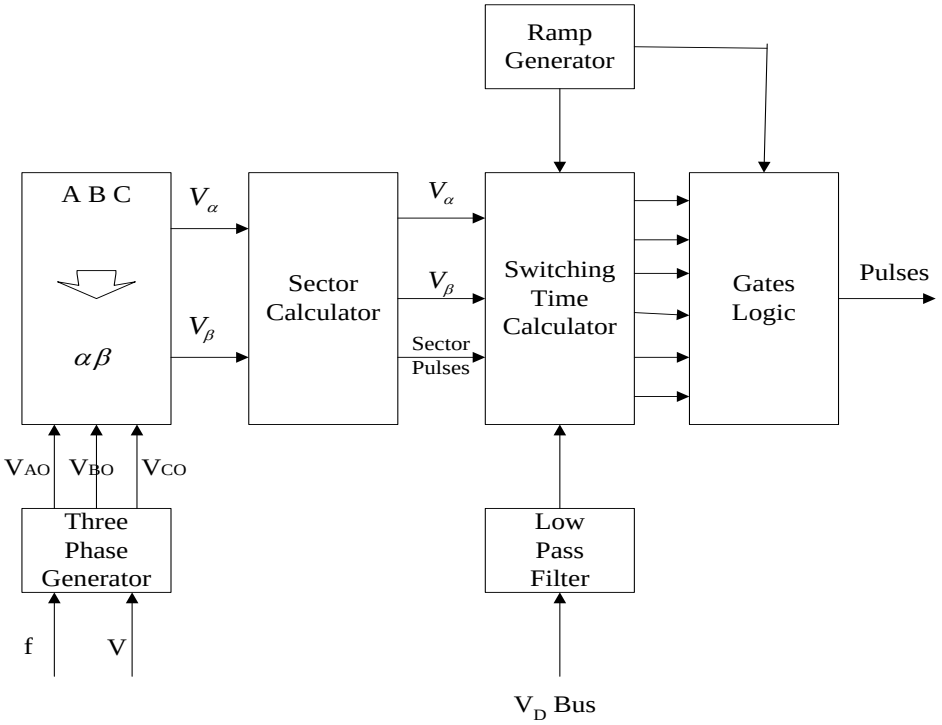


Fig.4.8 Operating Principle of SVM Generator

### 4.7.3 RESULTS AND DISCUSSION

The control scheme is simulated with Matlab/Simulink, for following case as:

- ❖ The speed reference prescribed to (800; 1000) rpm at t = (0; 1.5) s,
- ❖ The load torque prescribed to (0; 12) Nm at t = (0; 1.5) s with step variation.

The variations in time of the main electrical and mechanical variables are obtained, specific to the presented drive (the stator current $i_{sa}$, the rotor current $i_{ra}$, the rotor speed N and the electromagnetic torque Tem) and it represent them in Figure 4.9.

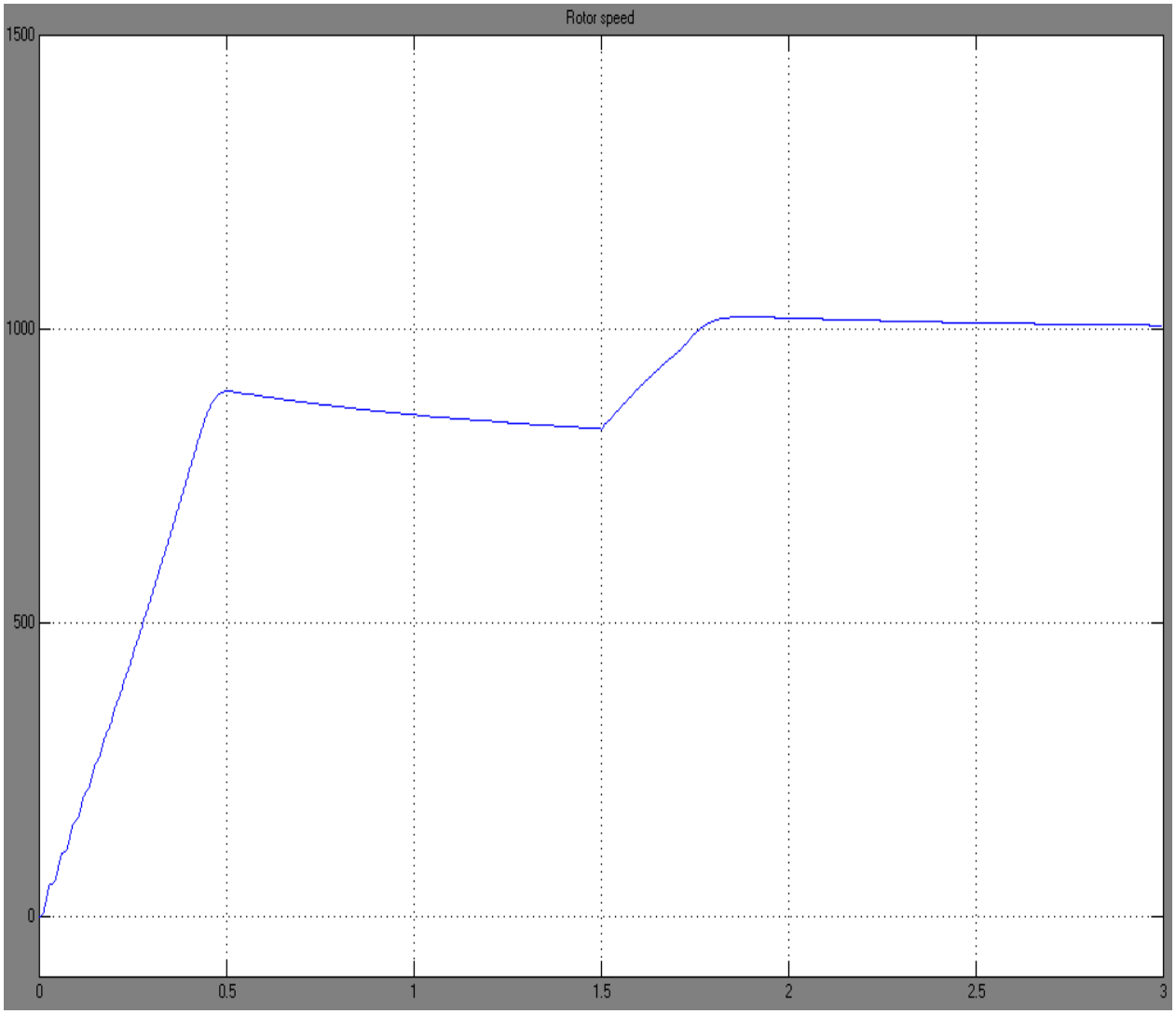


Fig 4.9 (a) Speed (rpm) v/s Time (second)

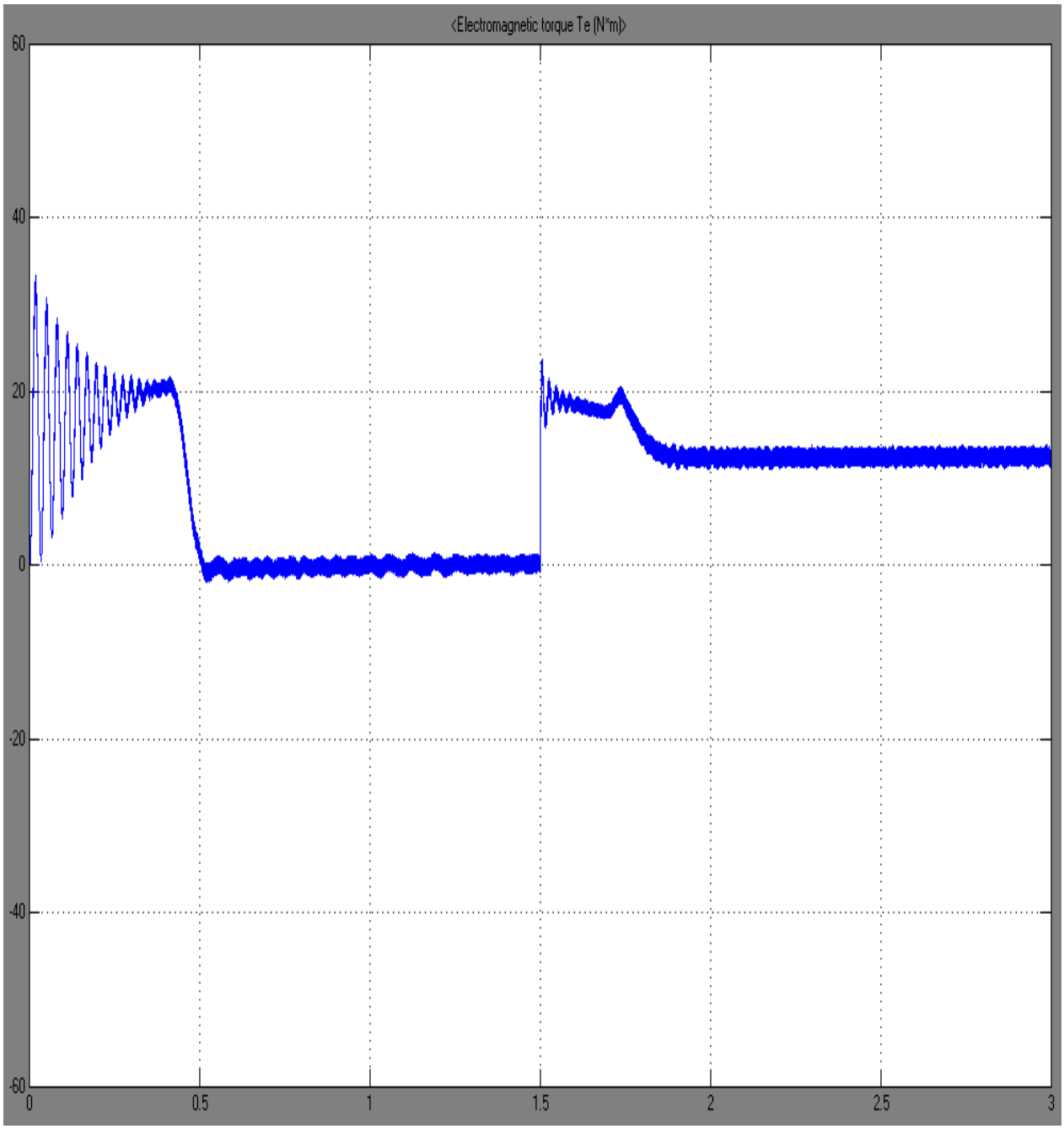


Fig 4.9(b) Torque (Nm) v/s Time (second)

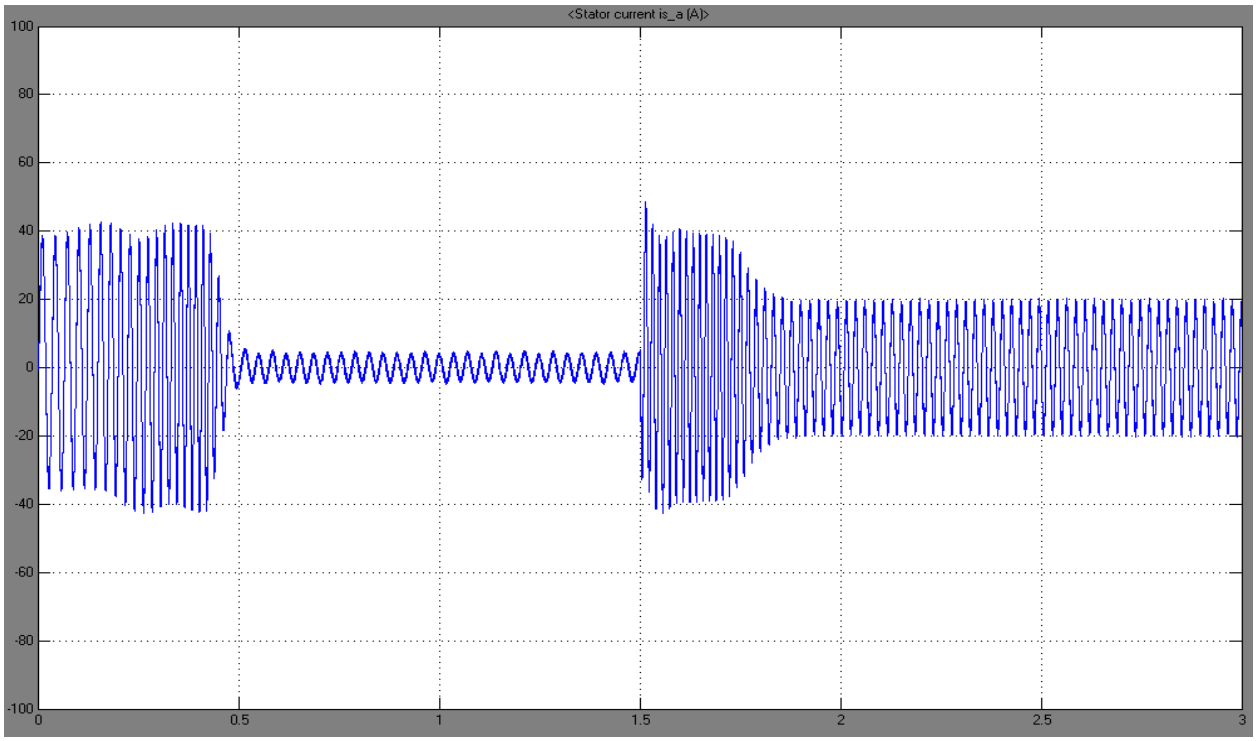


Fig 4.9(c) Stator Current (Ampere) v/s Time (second)

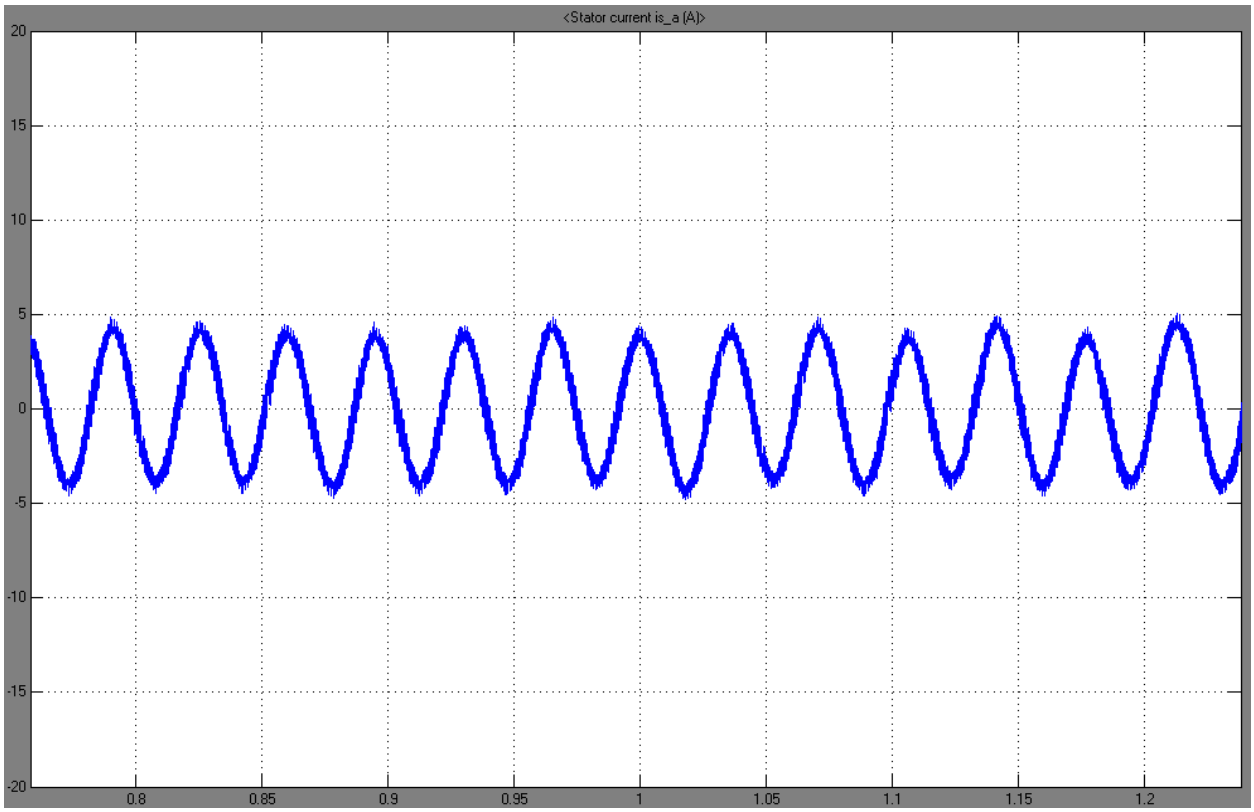


Fig 4.9(d) Stator Current (Ampere) v/s Time (second)

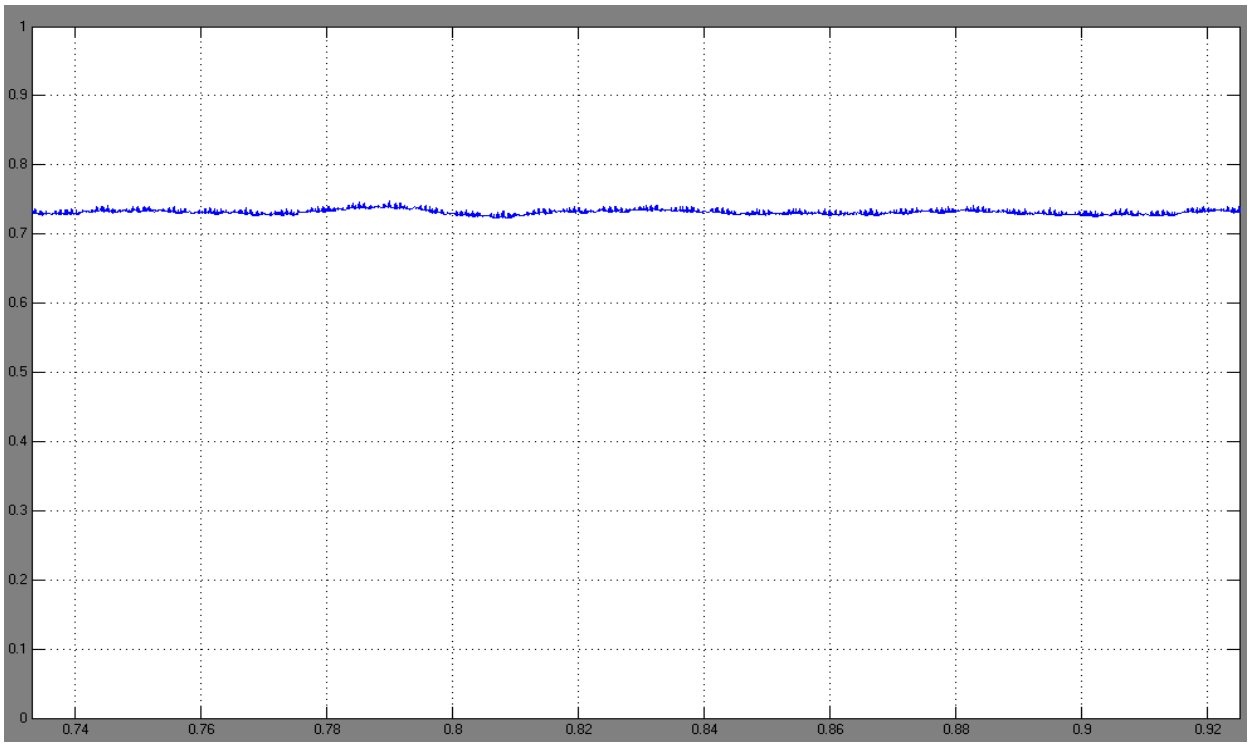


Fig 4.9(e) Stator Flux Linkage v/s Time (second)

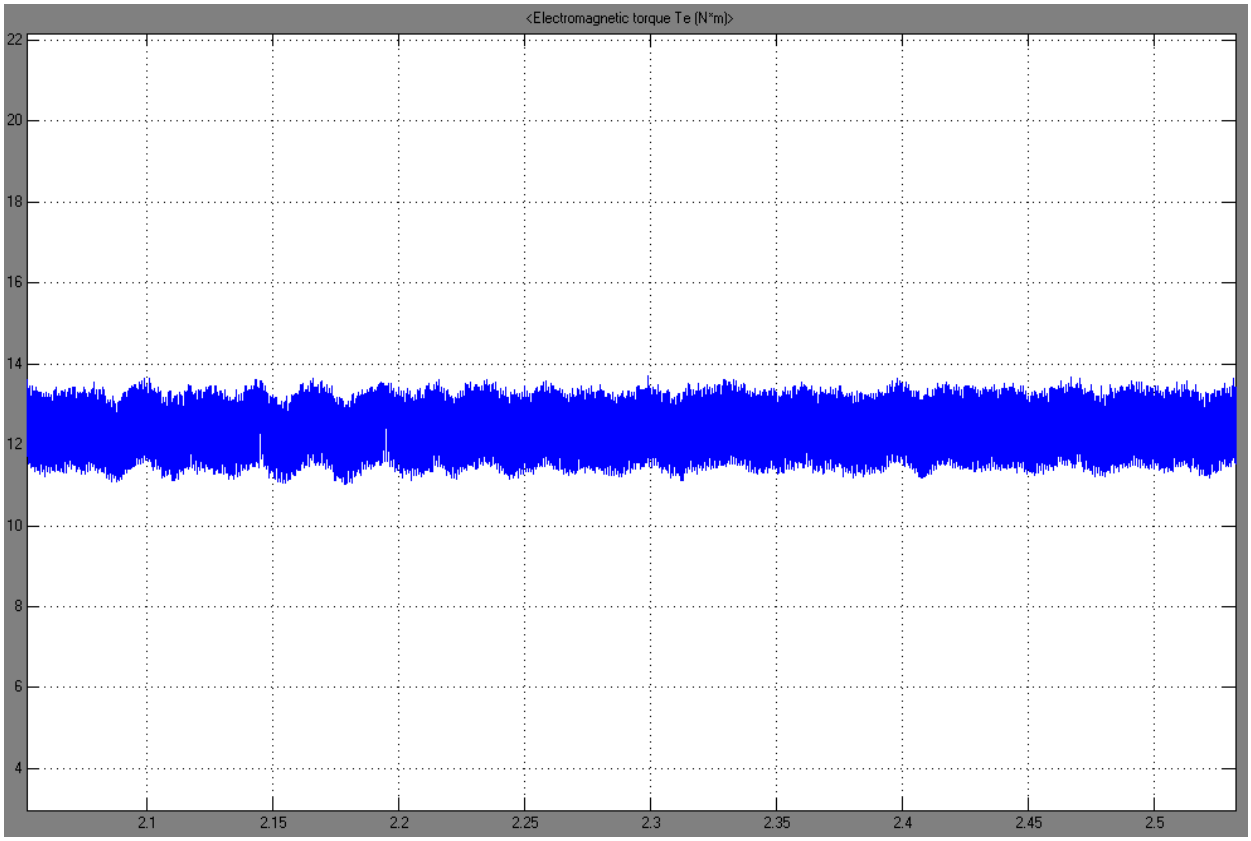


Fig.4.9(f) Torque Ripples in DTC-SVM

## 4.8 CONCLUDING REMARKS

- The Simulink model induction motor of variable speed control of induction motor is realized through the SVM strategy, using Simulink and Sim Power System blocks.
- The working model can be analyzing with accuracy, different electrical and mechanical variables.
- The SVM strategy provides fast torque response and than conventional DTC.
- Steady State torque ripples as well as the flux ripple are considerably reduced.
- The torque ripples in this technique is less compared to conventional DTC. As it can be seen from Figure 4.9(f), that the torque ripples present in DTC-SVM is ($\pm$ 1.5) Nm which is much less as compared to conventional DTC ($\pm$5) Nm.

# CHAPTER 5

# MAIN CONCLUSIONS AND FUTURE SCOPE

## 5.1 MAIN CONCLUSIONS

This work presents a comparative study of different direct torque control strategies of induction motor drive based on their simulation results. Space Vector Modulation direct torque control strategy is compared with the conventional direct torque control scheme.

Based on simulation results, it can be seen that the ripple in torque with SVM scheme is less than with conventional DTC. From the simulation results of DTC induction motor drive, the following conclusion can be made:

- Steady State torque ripple is considerably reduced. As from simulation results it can seen that the torque ripple present in DTC-SVM is ($\pm$1.5) Nm, which is much less as compared to conventional DTC ($\pm$5) Nm.
- Also the flux ripple is reduced considerably in this case.
- Ripple of stator current in the case of DTC-SVM has reduced.
- The switching frequency is constant and controllable in case of DTC-SVM.
- The performance of DTC-SVM can be further improved by appropriate tunning of the PI controller gains.

## 5.2 SCOPE FOR FUTURE WORK

- Torque ripples can also be reduced by applying the duty ratio controller.
- The performance of the classical DTC can be improved by neural network based DTC schemes.
- The simulation results can be validated by fabricating proto model.

# APPENDIX

Power Rating: 10 HP

Stator Voltage: 460 volt

Frequency: 60 Hz

Number of Poles: 4

Stator Resistance: 0.6837 ohm/phase

Stator leakage Inductance: 0.004152 H/phase

Rotor Resistance: 0.451 ohm/phase

Rotor leakage Inductance: 0.004152 H/phase

Mutual Inductance: 0.1486 H

Inertia: 0.05 kg $m^2$

Friction Coefficient: 0.0081412

# REFERENCES


[1] Krause P.C, "Analysis of Electrical machines and Drive systems", *Prentice Hall*, 1985.

[2] Bose B.K, "Modern power electronics and AC Drives", *Prentice Hall*, 2002.

[3] Rashid M.H., "Power Electronics Circuits, Devices and Applications", *Pearson Education, third Edition*, 2004.

[4] Abdul Wahab H.F. and Sanusi H., "Simulink Model of Direct Torque Control of Induction Machine", *American Journal of Applied Sciences* 5 (8): 2008, pp.1083-1090, ISSN 1546-9239 © 2008 Science Publications.

[5] Kang J.K., Sul S.K., "New Direct Torque Control of Induction Motor for Minimum Torque Ripple and Constant Switching Frequency". *IEEE Transactions on Industry Applications*, 35(5), 1999, pp.1076-1082.

[6] Nash J.N., "Direct torque control, induction motor vector control without an encoder", *IEEE Transactions on Industry Applications*, Vol.33, No.2, March/April 1997, pp.333–341.

[7] Casadei D., Serra G., Tani A., Zarri L. "Assessment of direct torque control for induction motor drives", Bulletin of Polish Academy of sciences, technical sciences, Vol.54, No.3, 2006.

[8] Schofield John R.G, "Direct Torque Control", ABB industrial systems Ltd., Institution of Electrical Engineers, 1995.

[9] Hoang L.H., "Comparison of field-oriented control and direct torque control for induction motor drives", Thirty-Fourth Industrial Applications Society Annual Meeting/Industry Applications Conference, Vol.2, October 1999, pp. 1245–1252.

[10] Marcel J., Ingo L., Liang Y., and Toni A., "Evaluation of vector and direct torque controlled strategies for cage rotor induction motor drives", *IEEE Transactions on Industry Applications*, Vol.1, August 2000, pp. 452–457.

[11] Jun Zhang, Rahman M.F., "Analysis and design of a novel direct flux control scheme for induction machine", Electric Machines and Drives, *IEEE International Conference on* 15 May 2005.

[12] Telford D., Dunnigan M.W., and Williams B.W., "A comparison of vector control and direct torque control of an induction machine", *Power Electronics Specialists Conference*, Vol.1, June 2000, pp.421–426.

[13] La K.K., Shin M.H., and Hyun D.S., "Direct torque control of induction motor with reduction of torque ripple", 26th Annual Conference of the *IEEE Industrial Electronics Society*, Vol.2, October 2000, pp.1082–1092.

[14] Farouk M. Abdel Kader, Saadawi A. E. L, Kalas A. E., Baksawi Osama M.E.L., "Study in direct torque control of induction motor by using space vector modulation", *IEEE Transactions*, 2008, pp.224-229.

[15] Choi Y.O., Lee K.Y., Seo K.S., Kim G.B., Jung B.H., Cho G.B., Baek H.L., and Jeong S.Y., "Performance analysis of the DTC using a closed loop stator flux observer for induction motor in the low speed range", Proceedings of the Fifth International Conference, Electrical Machines and Systems, Vol.1, August 2001, pp.89–93.

[16] Toh C.L., Idris N.R.N., Yatim A.H.M., "Torque ripple reduction in direct torque control of induction motor drives", Power Engineering Conference, Proceedings National 15-16 Dec. 2003.

[17] Krishnan R. "Electric Motor Drives-Modelling, Analysis and Control", *Prentice Hall*, 2001.

[18] Lee B.S., and Krishnan R., "Adaptive stator resistance compensator for high performance direct torque controlled induction motor drives", *IEEE Industry Applications Conference*, Vol.1, October 1998, pp. 423–430.

[19] Wang Y., Lu J., Huang S., and Qiu S., "Speed sensor less vector control of induction motor based on the MRAS theory", Power Electronics and Motion Control Conference, Vol.2, August 2004, pp. 645–648.

[20] Seyoum D., Grantham C., and Rahman M.F., "Simplified flux estimation for control application in induction machines", *IEEE International Electric Machines and Drives Conference*, Vol.2, June 2003, pp. 691–695.

[21] Casadei D., Serra G. and Tani A., "Constant frequency operation of a DTC induction motor drive for electric vehicle", *Proc. ICEM '96 Conf.* 3, 1996, pp.224–229.

[22] Kim S.H., Sul S.K. and Park M.H., "Maximum torque control of an induction machine in the field weakening region", *Conf. Rec. IEEE-IAS'93* 1, 1993, pp.401–407.

[23] Lascu C., Boldea I., and Blaabjerg F., "Variable-structure direct torque control—a class of fast and robust controllers for induction machine drives", *IEEE Transactions on Industry Electron*, Vol.51, August 2004, pp.785–792.

[24] Ohtani T., Takada N. and Tanaka K., "Vector control of induction motor without shaft encoder", *IEEE Transaction on IA.* Vol.28, No.1, Jan/Feb. 1992, pp.157-164.

[25] Tajima H. and Hori Y., "Speed sensorless field-oriented control of the induction machine", *IEEE Transactions on Industry Applicaions*, Vol.29, Jan./Feb. 1993, pp.175- 180.

[26] Casadei D., Grandi G. and Serra G., "Study and implementation of a simplified and efficient digital vector controller for induction motors", *Conf. Rec. EMD'93*, 1993, pp.196–201.

[27] Tiitinen P., Pohkalainen P. and Lalu J. "The next generation motor control method: direct torque control (DTC)", *EPE J.* 5 (1), 1995, pp.14–18.

[28] Vas P., *Sensorless Vector and Direct Torque Control*, Clarendon Press, 1998.

[29] Masood H., Jafar S., Gholamreza A. M. and Saeed H., "Adaptive Non-Linear Direct Torque Control Of Sensorless Induction Motor Drives With Efficiency Optimization", *IEEE Transactions on Industrial Electronics*, Vol.57, No.3, March 2010.

[30] Tang, L., and Rahman, M.F., "A new direct torque control strategy for flux and torque ripple reduction for induction motors drive by using space vector modulation", *Power Electronics Specialists Conference*, Vol.3, June 2001, pp.1440–1445.

[31] Yongheng L., Xiaoyun F., Xiaohao Z., Yanzhi W., "Research And Simulation on Constant Switching Frequency Of Direct Torque Control (DTC)", Southwest Jiao Tong University, Chengdu, 610031, China, 2010.

[32] Daniel M.S., Garcia Escudero L.A., Oscar D.P., and Marcelo P. A., "Practical Aspects of Mixed-Eccentricity Detection in PWM Voltage-Source Inverter-Fed Induction Motor", *IEEE Transactions on industry electronics*, Vol.57, No.1, Jan. 2010.

[33] Rodriguez, J.; Pontt, J.; Silva, C.; Kouro, S.; Miranda, H.; "A novel direct torque control scheme for induction machines with space vector modulation", Power Electronics Specialists Conference, PESC 04, *IEEE 35th Annual*, Vol.2, 20-25 June 2004 .

[34] Savulescu A., "Aspects Of Variable Speed Control Of Asynchronous Motors Through The Technique Of Space Vector Modulation", 6th International Conference on Electromechanical and Power Systems in Chisinau, Rep.Moldova, October 4-6, 2007.

[35] Elbuluk, M., "Torque ripple minimization in direct torque control of induction machines", *IEEE Industry Applications Conference*, Vol.1, No. 2, October 2003, pp.11–16.

[36] Ershadi M.H., Moallem M. and Ebrahimi M., "Loss-minimization scheme in modified DTC-SVM for induction motors with torque ripple mitigation", Journal of Applied sciences Vol.10, No.19, 2010, pp.2269-2275, ISSN 1812-5654 © 2010 Science Publications.

[37] Kumar P. Satish, Amarnath J. and Narasimham S.V.L., "An Effective Space-Vector PWM Method For Multi-Level Inverter Based On Two-Level Inverter", *IEEE International Journal*, Vol.2, No.2, April 2010, pp.1793-8163.

[38] Abdelnassir, A., "Torque Ripple Minimization in Direct Torque Control of Induction Machines", Masters Thesis, University of Akron, Akron, Ohio, May 2005.

[39] Haghbin, S., Zolghadri, M. R., Kaboli, S., and Emadi, A., "Performance of PI stator resistance compensator on DTC of induction motor", Industrial Electronics Society, *29th Annual Conference of the IEEE*, Vol.1, November 2003, pp. 425–430.

[40] Mei C. G., Panda S. K., Xu J. X., Lim K. W., "Direct Torque Control of Induction Motor-Variable Switching Sectors", *IEEE International Conference on Power Electron and Drive Systems PEDS* in Hong Kong, 1999, pp. 80-85.

[41] Casadei D., Grandi G., Serra G. and Tani A., “Effects of flux and torque hysteresis band amplitude in direct torque control of induction machines”, *Conf. Rec. IECON’94*, 1994, pp.299–304.

[42] Casadei D., Grandi G., Serra G. and Tani A. “Switching strategies in direct torque control of induction machines”, *Conf. Rec. ICEM’94*, 1994, pp.204–209.

[43] Kaboli S., Vahdati Khajeh E. and Zolghadri M.R., “Probabilistic voltage harmonic analysis of direct torque controlled induction motor drives”, *IEEE Transactions on Power Electronics*, Vol.1, No.4, 2006, pp.1041–1052.

[44] Escobar G., Stankovic A.M., Galvan E., Carrasco J.M. and Ortega R.A., “A family of switching control strategies for the reduction of torque ripple in DTC”, *IEEE Transactions on Control Systems Technology*, Vol.11, No.6, 2003, pp.933–939.

[45] Habetler T.G., Profumo F., Pastorelli M. and Tolbert L.M., “Direct torque control of induction machines using space vector modulation”, *IEEE Transactions on Industrial Applications*, Vol.28, September/October 1992, pp.1045–1053.

[46] Hamid Reza Keyhani, Mohammad Zolghadri, Abdollah Homaifar. "An extended and Improved Discreate Space Vector Modulation Direct Torque Control for Induction Motors", 35th Annual IEEE Power Electronics Specialists Conference 2004.

[47] Xin Wei, Dayue Chen, Chunyu Zhao. "Minimization of torque ripple of direct torque controlled induction machines by improved discrete space vector modulation", Electric Power systems Research 72, 2004, pp.103-112.

[48] Martins C.A., Roboam X., Meynard T.A. and Carvalho A.S., “Switching frequency imposition and ripple reduction in DTC drives by using a multilevel converter”, *IEEE Transactions on Power Electronics* Vol.17, No.2, 2002, pp.286–297.

[49] Lee K.B., Song J.H., Choy I., Choi J.Y., Yoon J.H. and Lee S.H., “Torque ripple reduction in DTC of induction motor driven by 3-level inverter with low switching frequency”, *PESC 00* 1, 2000, pp.448–453.

[50] Lai Y.S. and Chen J.H., “A new approach to direct torque control of induction motor drives for constant inverter switching frequency and torque ripple reduction”, *IEEE Transactions on Energy Conversion*, Vol.16, No.3, 2001, pp.220–227.

[51] Habetler T.G., Profumo F., Pastorelli M. and Tolbert L.M. "Direct torque control of induction machines using space vector modulation", *IEEE Transactions on Industrial Applications*, Vol.28, September/October 1992, pp.1045–1053.

[52] Wu, J., Li, Y., Chen, J., and Hu, H., "Speed sensor-less direct torque control of an induction machine in low speed region," Power Electronics and Motion Control Conference, Vol.1, August 2000, pp.464–468.

[53] Boldea I. and Nasar S.A. "Torque vector control (TVC)-A class of fast and robust torque speed and position digital controller for electric drives", *Proc. EMPS'88 Conf.* 15, 1988, pp.135–148.

[54] Lascu C., Boldea I., Blaabjerg F., "A modified direct torque control for induction motor sensorless drive", *IEEE Transactions on Industrial Applications*, Vol.36, No.1, 2000, pp.122-130.

[55] Takahashi and Ohmori Y. "High-performance direct torque control of an induction motor", *IEEE Transactions on Industrial Applications*, Vol.25, 1989, pp.257–264.

[56] Wu X.Q. and Steimel A., "Direct self control of induction machines fed by a double three-level inverter", *IEEE Transactions on Industrial Electronics*, Vol.44, No.4, 1997, pp.519–527.